EFFECTS OF CONVECTION ON MASS AND MOMENTUM FIELDS AS SEEN FROM CLOUDSCALE SIMULATIONS OF PRECIPITATING SYSTEMS

J.–P. Lafore and J.–L. Redelsperger
(CNRM/METEO–FRANCE and CNRS)

1. INTRODUCTION

Virtually everything in large scale models is sensitive to convection and it is therefore crucial to represent it properly. It is a very difficult task, and progress can only be achieved by concerted studies based on observations, models and theory. During the ECMWF workshop on diabatic forcing, Houze (1987) summarized the structure of mesoscale convective systems and the associated vertical distribution of diabatic heating as derived from field experiment observations. Such approach to diagnose the effect of convection have been of great benefit to the validation and development of convective schemes. However, the amount of observational data is small and convective schemes have been verified only against a limited number of experimental cases. The topic of the today workshop clearly wants to proclaim that the fine-scale modelling art has now reached a sufficient mature stage to bring an useful contribution to the parameterization problem. In this paper we will show the ability of such models to help to this difficult task, and propose a strategy to progress in that direction.

We chose to illustrate the potentialities of fine-scale modelling allowing an explicit resolution of the convection, on two very different flow regimes. The first one concerns a fast-moving Tropical squall-line observed on the 22 June during the COPT81 (Sommeria and Testud, 1984) experiment, and for which the unbalanced part of the flow dominates. The strongly balanced flow case, will be illustrated by recent two-dimensional simulations of the frontal system observed on the 11 September during the European MFDP/FRONTS87 experiment (Browning *et al.*, 1986; Clough and Testud, 1988). In section 2.1, some results of the extensive comparisons between the simulations and field observations (including Doppler radar data) will demonstrate the ability of such fine-scale models to realistically simulate convection. An important consequence of this agreement between simulations and observations, is the possibility of using simulation results to compute water (section 2.2), heat, moisture (section 2.3) and momentum (section 2.4) budgets and vertical transports, to study the effects of convection at larger scale and discuss its parameterization.

The section 3 follows the same way but for the frontal case. We will conclude in

section 4, with a general discussion on both systems types and some recommendations.

2. THE TROPICAL SQUALL LINE CASE

The two and three-dimensional simulations of squall line presented in this paper have been performed with the anelastic, deep convection model of Redelsperger and Sommeria (1986). The current version contains eight prognostic equations: the three momentum equations, the thermodynamic equation, three water conservation equations (water vapor, liquid cloud water, and rain water), and a subgrid kinetic energy equation. The pressure is obtained diagnostically. A bulk type parameterization of solid hydrometeors as been recently implemented (Caniaux *et al.*, 1991) to represent cloud ice, aggregates and graupels fields.

2.1 Comparisons with observations

Three-dimensional convective scale simulations of an African squall line, observed during the french COPT 81 experiment, have been performed on a domain of 50 km (along the line) by 80 km (across the line) and 23 km in the vertical (Redelsperger and Lafore, 1988; RL88 hereafter). After 6 h of simulation a quasi-steady squall line is obtained whose global characteristics, like the propagation speed (14 m s^{-1}) and total rain-rate (20000 t s^{-1} over the whole domain), indicate good agreement with field observations. To validate more fully the model, the dynamical fields have been extensively compared (Lafore *et al.*, 1988; LRJ88 hereafter) with Doppler radar three-dimensional wind fields. The comparisons use a two-dimensional statistical analysis, in which each four-dimensional field is decomposed into the sum of a two-dimensional averaged vertical field and a four-dimensional residual field, representating along-line and temporal fluctuations. Figures 1 show examples of such comparisons for the vertical velocity w field. Staying in the moving system frame, the warm and wet air of the 2 km deep monsoon layer rapidly enters the system (left of the pictures). This unstable air is then transported upward by a main updraft, where a large amount of latent heat is released by condensation. Outside this region, subsident motion develops. Both radar and model find the same structure (Figs. 1a, 1b) for its shape and intensity. The standard deviation of temporal and along-line fluctuations of w (Figs. 1c, 1d) also indicate good agreement. Their relative importance demonstrate the fully three-dimensional and transient nature of the convective cells, where intense updrafts (up to 35 m s^{-1}) cross subsident dry air (up to -10 m s^{-1}). Similar comparisons have been performed for the line-normal along-line wind and vertical fluxes of line-normal momentum and indicate good agreement.

To study the whole system, we have also performed two-dimensional simulations on a large domain (500 km) and with a solid and liquid-water parameterization (Caniaux

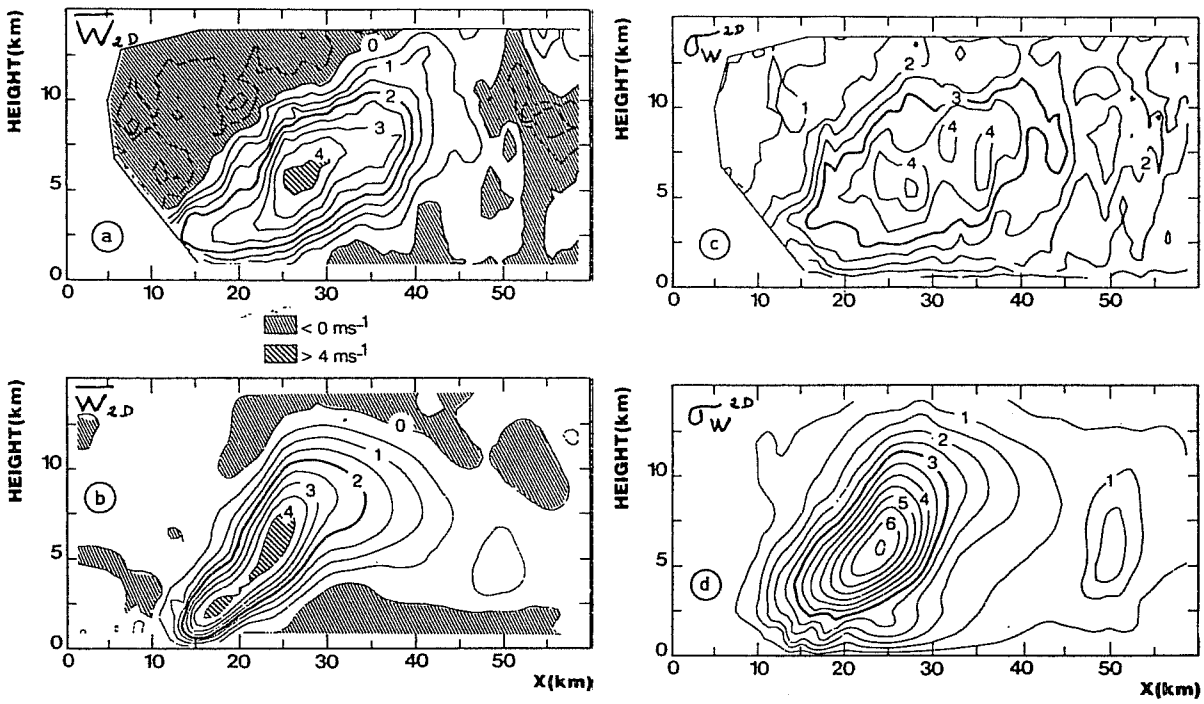

Fig. 1: Two-dimensional analysis of vertical velocity in the convective part of the squall line case.

(a) Two-dimensional average for Doppler radars. Downdraft areas are dashed, and areas with values larger than 4 m s^{-1} are heavily dashed. The heavy line represents the 2 m s^{-1} isoline. (b) As (a) but for the simulation.

(c) Total standard deviation but for radars. The heavy line represents the 3 m s^{-1} isoline. (d) As (c) but for the simulation. (From Lafore et al., 1988)

et al., 1991 a and b). The quasi-steady state reached (Fig. 2) reproduces many features observed by Chalon *et al.*, (1988) (Figs. 3), with four identified regions: a 40 km wide convective part, a well-developed stratiform zone over 120 km with moderate precipitation (1 to 10 mm h^{-1}), a transition region with light precipitation and a forward anvil. The "rear inflow" jet, the bright band due to melting of ice particles, the cold pool spreading at the ground are also in agreement with observations. The vertical motion pattern in the stratiform part is well reproduced (Figs. 2c and 3c), with a mean ascent in the mid troposphere and subsident motion underneath. It should be noticed that without ice phase parameterization, the system does not succeed to develop this extended trailing anvil.

In the convective zone, the vertical velocities are less realistic with two strong updrafts separated by nearly zero velocity values. In this strongly transient region (as indicated by high temporal variance of w), the cells cannot properly develop upward, as corresponding to strong environmental air mixing. This feature is thought to be the result of two-dimensional framework, as supported by the realistic simulation of this part obtained by RL88 in a three-dimensional framework.

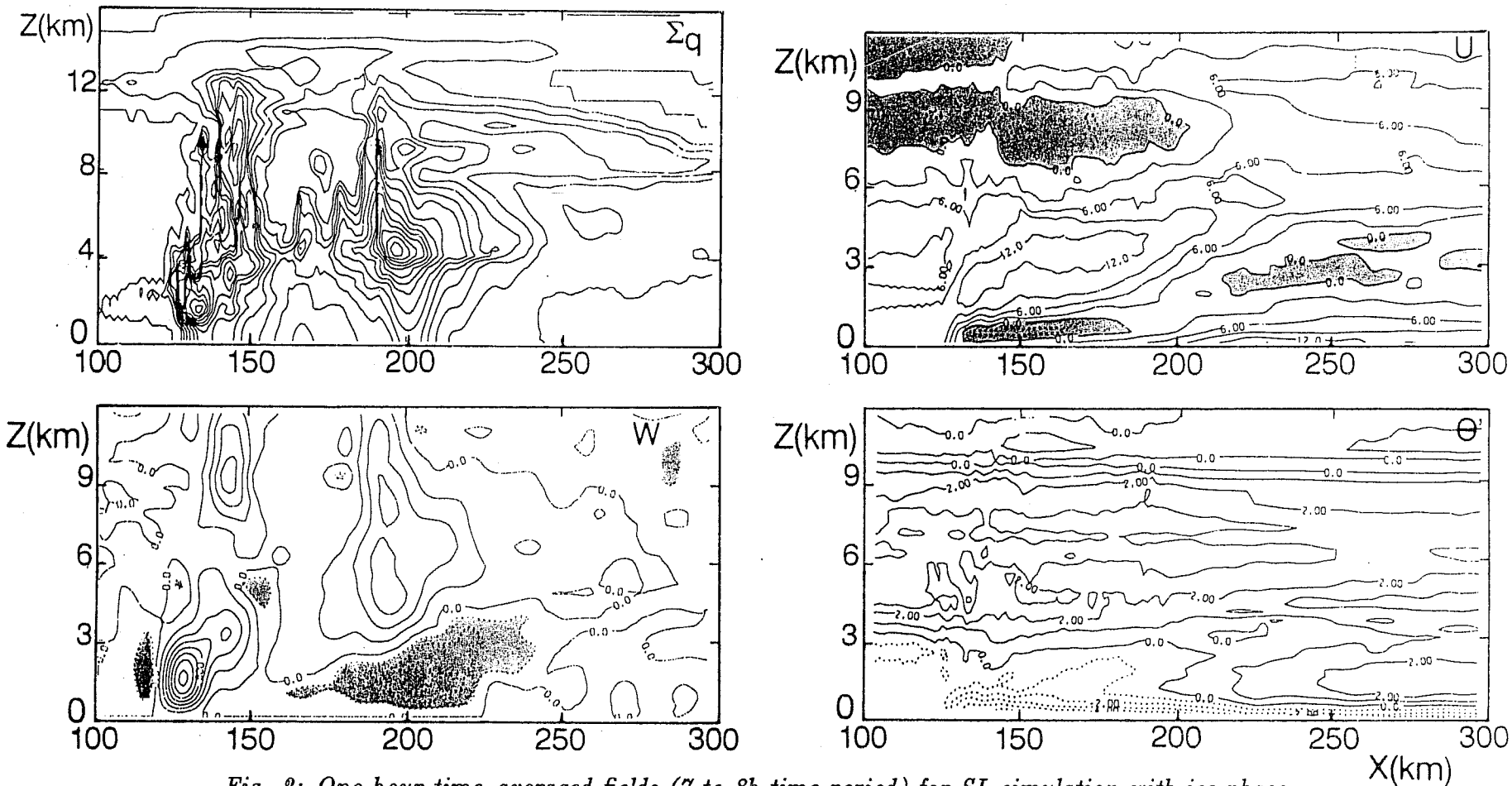

Fig. 2: One hour time-averaged fields (7 to 8h time period) for SL simulation with ice phase (a) the total liquid and ice water content (the contour interval is 10^{-4} g g^{-1} and the maximum value is 1.45 10^{-3} g g^{-1}), (b) the horizontal wind relative to translation speed of the model frame (-12 m s^{-1}) (contour interval of 3 m s^{-1}), (c) the vertical velocity (contour interval is .2 m s^{-1} for upward velocities (solid lines) and .1 m s^{-1} for downward velocities), (d) and the temperature perturbation (the contour interval is 1°C, minimum and maximal values are -5.5 and 4.5°C).

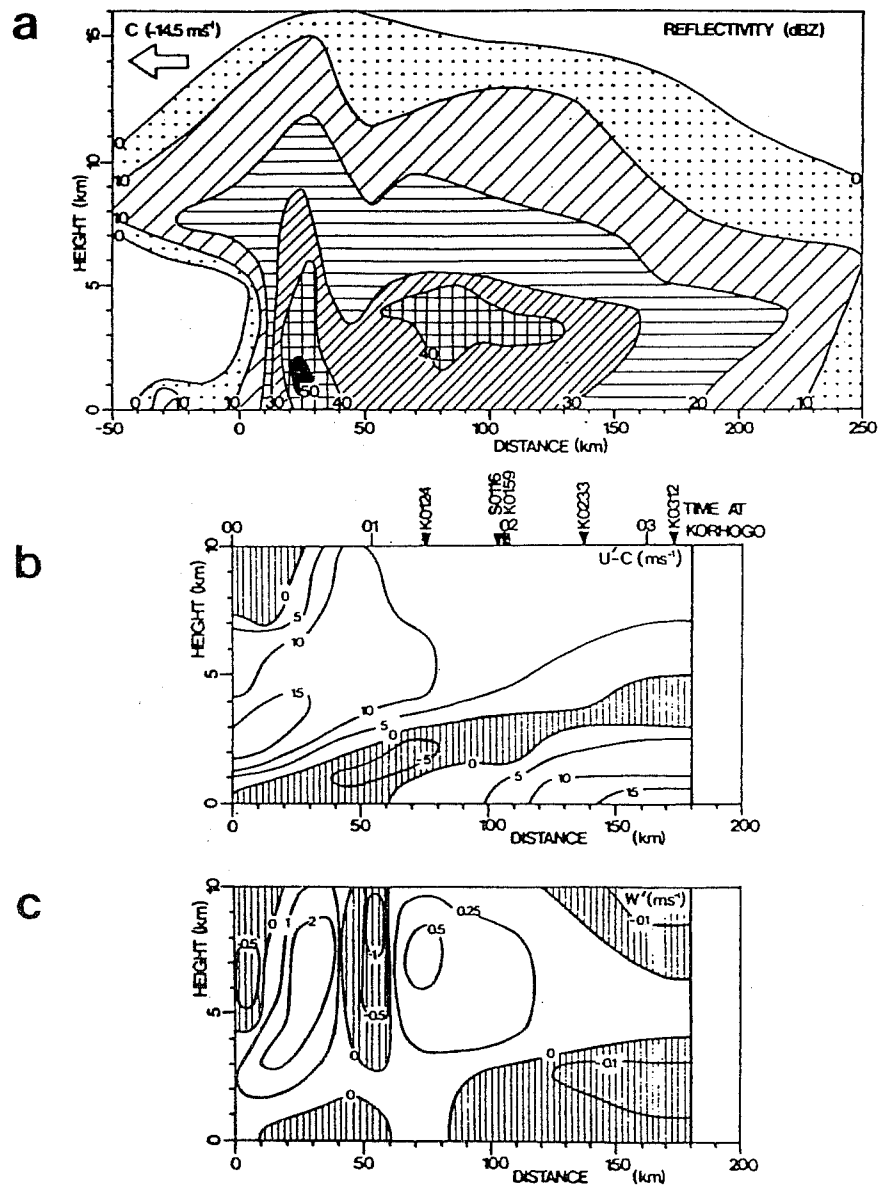

Fig. 3: Vertical cross sections of mesoscale composites of (a) radar reflectivity (in dBZ), (b) cross-line wind component relative to the SL, and (c) vertical velocity (all in ms^{-1}). (From Chalon et al., 1988).

2.2 Water budget

The water budget have been studied in detail for the two-dimensional simulation of the squall line case (Caniaux *et al.*, 1991 (a)). The budget of total condensated water q can be expressed as :

$$\frac{dq}{dt} = COND_c - RR - EVAP_R + Flux_e - Flux_s$$

where RR is the surface precipitation in the considered box, $Flux_e$ is the inflow of condensate and $Flux_s$ the outflow one. $EVAP_R$ is evaporation of rainwater in the

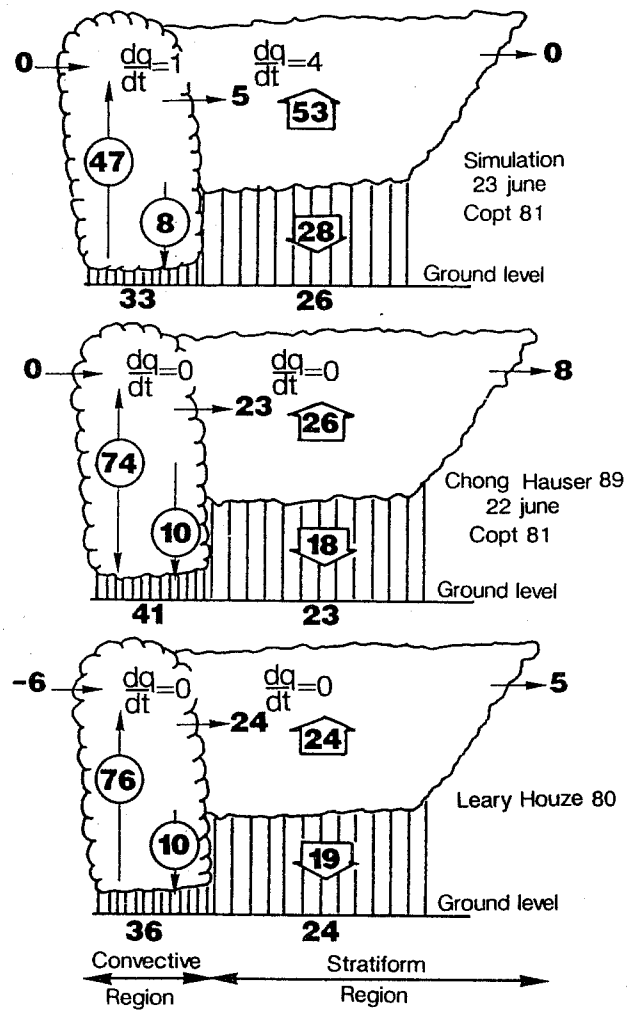

Fig. 4: Schematic diagram of the squall-line water budget for simulations of Caniaux et al.(1991), and for observations of Chong and Hauser (1989) and Leary and Houze (1980).

convective or mesoscale downdrafts and $COND_c$ is the net condensation term, both including condensation/deposition and evaporation of cloud liquid water and sublimation. This term is so computed to be compared with observational water budget. A storage term has to be introduced ($\frac{dq}{dt}$) if the system is not considered in a steady state.

Results expressed as percentage of total condensation are compared with observations of Chong and Hauser (1989) and Leary and Houze (1980) on (Fig. 4). For the present purpose, the main conclusions are:

- Condensation in the convective part is weaker than observed, due to overestimated cloud evaporation obtained in a two-dimensional framework. The two-dimensional simulation underestimates the convective contribution (56 % of the total precipitation, instead of 80 % observed for this case) contrary to the three-dimensional simulation giving the right amount of precipitation in the convective part. Therefore the budget

calculation confirms the larger realism of the convective part in the three–dimensional framework than in the two–dimensional one.

- In the stratiform region, the water budget is similar to the one deduced from observations of tropical fast moving squall-lines. Examination of this budget stresses the importance of the mesoscale updraft in producing more condensate than what is advected from the convective box. The stratiform part contributes for 20 to 40 % to the total precipitation at the ground.

2.3 Heat and moisture apparent sources

2.3.1 The formalism including fusion

The equations of the cloud model can be related to both the apparent heat source Q_1 and apparent moisture sink Q_2, by horizontally averaging the thermodynamic and water vapor equations, yielding to:

$$Q_1 \equiv \langle\pi\rangle\langle\frac{D\theta}{Dt}\rangle = -\frac{\langle\pi\rangle}{\langle\rho\rangle}\langle\frac{\partial\langle\rho\rangle w'\theta'}{\partial z}\rangle + Q^* + D_{Q_1} \tag{1}$$

$$Q_2 \equiv -\frac{\langle L\rangle}{C_p}\langle\frac{Dq_v}{Dt}\rangle = \frac{\langle L\rangle}{C_p\langle\rho\rangle}\langle\frac{\partial\langle\rho\rangle w'q_v'}{\partial z}\rangle + Q + D_{Q_2} \tag{2}$$

where $\pi = \frac{T}{\theta}$, D_{Q_1} and D_{Q_2} are the subgrid scale diffusion, brackets denote horizontal averages and $'$ the deviations from horizontal averages. Q^* is the total latent heating including both condensation, sublimation and fusion and Q only refer to vapor heat release (i.e. condensation and sublimation). Writing $Q^* = Q_i + Q$, we should note that in general $Q \gg Q_i$, since fusion latent heating is one order smaller than vaporisation latent heating (L). Q_i is thus a residual term added to Q for computation of Q_1 and will indicate the ice phase contribution to the Q_1 budget.

2.3.2 The partitioning

A partitioning method is used to analyse the contribution of convective and stratiform parts, to the total Q_1 and Q_2 terms averaged on the system scale. Each model variable X averaged on the system scale ($\overline{X}$), is writen as:

$$\overline{X} = \alpha_c\overline{X}^c + \alpha_m\overline{X}^m \tag{3}$$

where $\overline{X}^c$ and $\overline{X}^m$ are spatial averaging on the convective and stratiform boxes respectively. α_c and α_m refer to the fraction of total length $L_c + L_m$ covered by convective and stratiform regions (i.e. $\alpha_c = \frac{L_c}{L_c+L_m}$ and $\alpha_m = \frac{L_m}{L_c+L_m}$). Due to the non-linear term

of vertical transport in the Q_1 and Q_2 equations, a supplementary term must be added to the partitioning average (Eq. 3). Either:

$$\overline{Q_1} = \alpha_c \left[\overline{Q_1}^c - \frac{\langle \pi \rangle}{\langle \rho \rangle} \frac{\partial}{\partial z} (\langle \rho \rangle \overline{\langle w \rangle}^{*c} \overline{\langle \theta \rangle}^{*c}) \right] + \alpha_m \left[\overline{Q_1}^m - \frac{\langle \pi \rangle}{\langle \rho \rangle} \frac{\partial}{\partial z} (\langle \rho \rangle \overline{\langle w \rangle}^{*m} \overline{\langle \theta \rangle}^{*m}) \right] \quad (4)$$

where $\overline{w}^{*c}$ ($\overline{w}^{*m}$ etc...) represent the deviation between the mean value on each box (c or m) and the mean value on the whole system. An identical formulation is used for Q_2 budget.

2.3.3 Three-dimensional simulation of the convective part

LRJ88 computed the Q, Q_1 and Q_2 terms from the three-dimensional convective part simulation of RL88. The Q_i term is zero in that case, as solid water was not parameterized.

The latent heating (Fig. 5a) provides a good approximation of the apparent heating source Q_1 (Fig. 5b); nevertheless, computation of this latent heating should include rain evaporation. The computation of the apparent moisture sink Q_2 (Fig. 5c) necessitates that of its convective eddy transport. The transport due to convective eddies decouples the vertical distributions of heat and moisture. The normalization by the rainfall rate (Johnson, 1984) allows to successfully compare the simulated Q_1 and Q_2 terms (Fig. 6) with previous diagnostic studies with larger time and space scales. The double-peak structure of Q_2 profile often seen in tropical budget composite studies, is confirmed. In this study, this moistening peak appears in the convective part as an effect of the strong convergence of moisture transport by convective eddies at upper levels (Fig. 5c).

2.3.4 Two-dimensional simulation of the whole system

The Q, Q_1 and Q_2 are now computed from the two dimensional squall-line simulation, including the ice phase parameterization. The partitioning technique is used with a spatial averaging $L_c = 50$ km and $L_m = 250$ km for the convective and stratiform boxes respectively, and averaged over one hour of simulation. The main conclusions obtained by LRJ88 for the convective part are confirmed.

The latent heating profiles Q are shown on Fig. 7. Latent heating in the convective part is weak and occurs on a too shallow depth due to the enhanced cloud evaporation. The stratiform region is marked by heating in the midlevels with a maximum near 6 km and by cooling at lower levels. The heating is mainly due to condensation and deposition occurring in the mesoscale ascent. The cooling corresponds to rain evaporation in the mesoscale subsidence. The melting layer is well marked in the stratiform part. However,

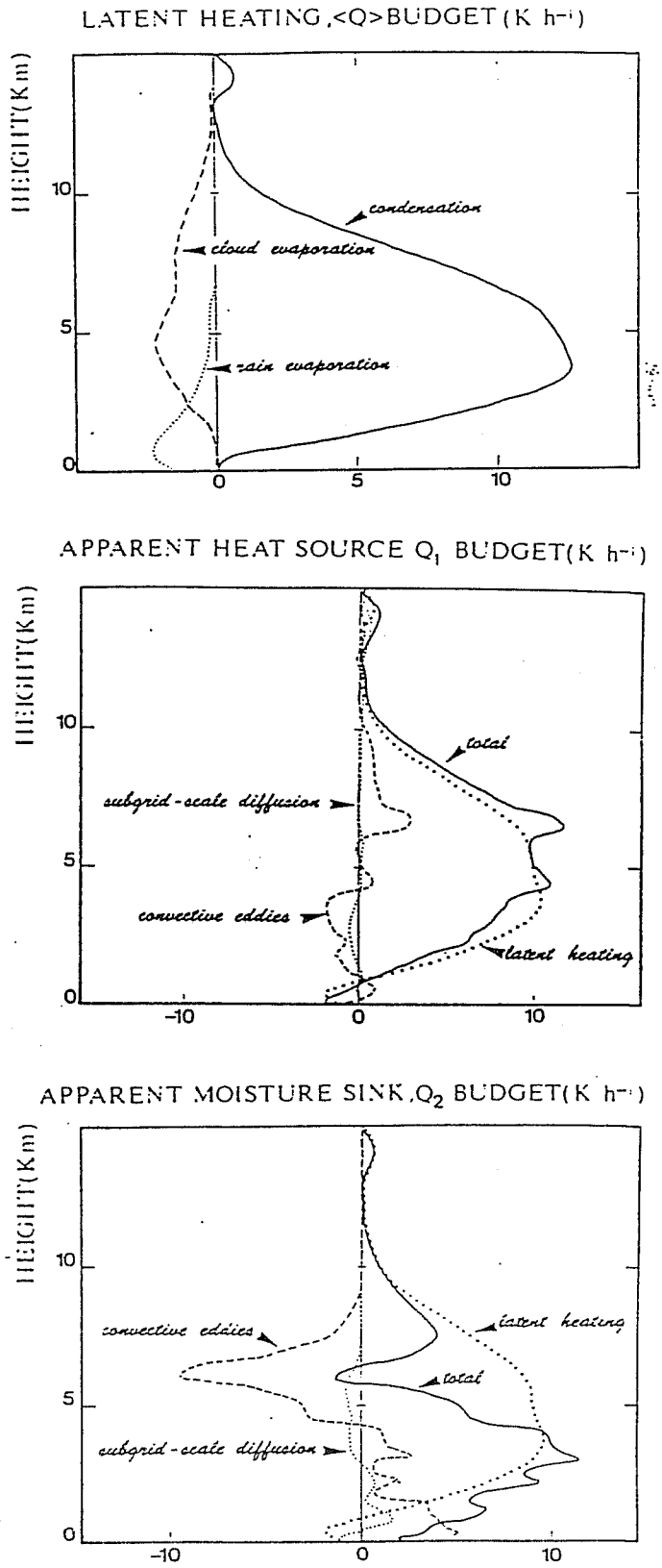

Fig. 5: Vertical profiles of (a) latent heating Q, (b) apparent heat source Q_1, and (c) apparent moisture sink Q_2, for the simulated convective part of the squall line. (From Lafore et al., 1988)

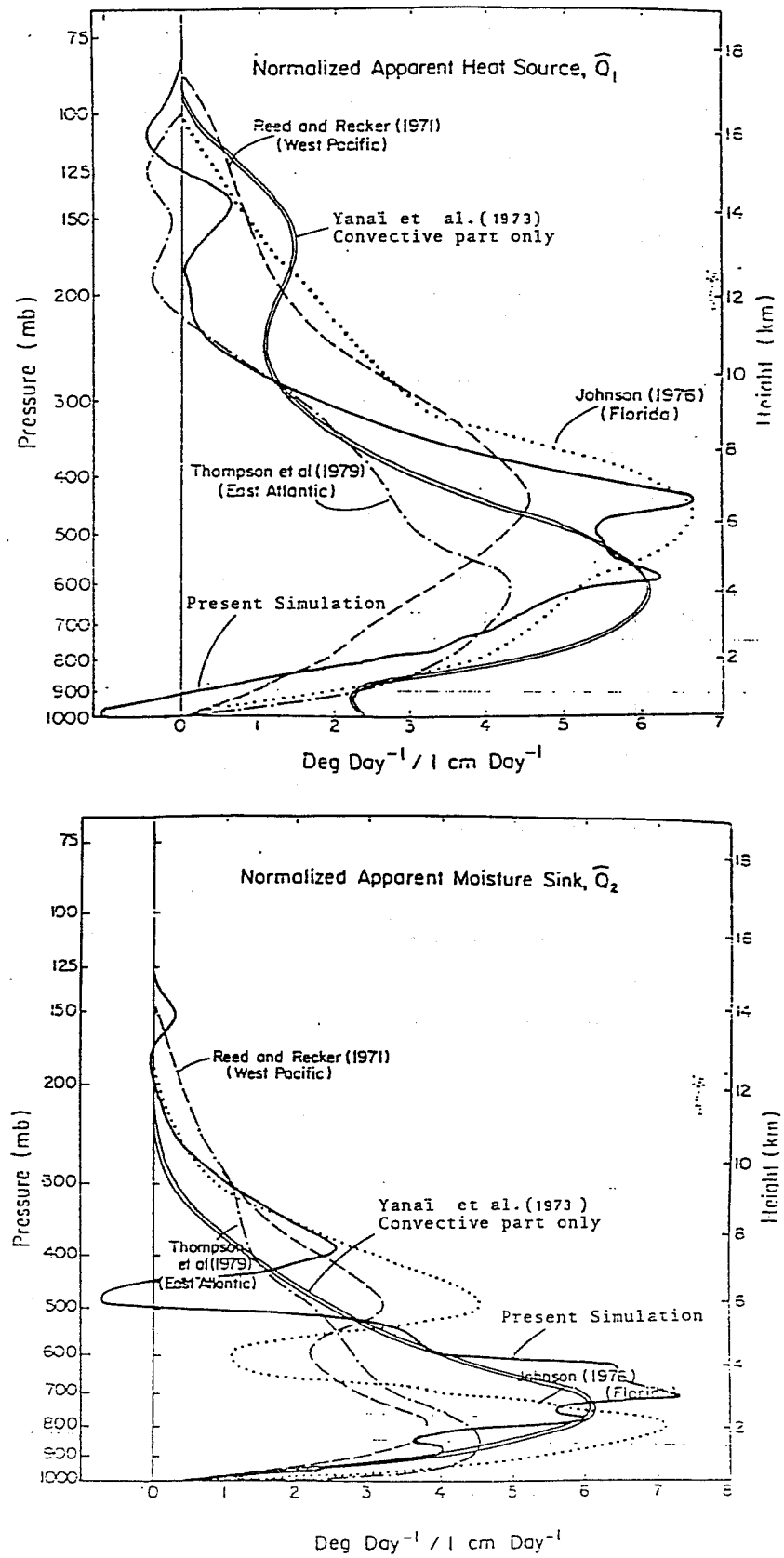

Fig. 6: Normalized apparent heat source $\hat{Q}_1$ (a), and normalized apparent moisture sink $\hat{Q}_2$ (b), for observations in West Pacific, East Atlantic, and Florida regions, and for the simulated convective part of the squall line. (From Lafore et al., 1988)

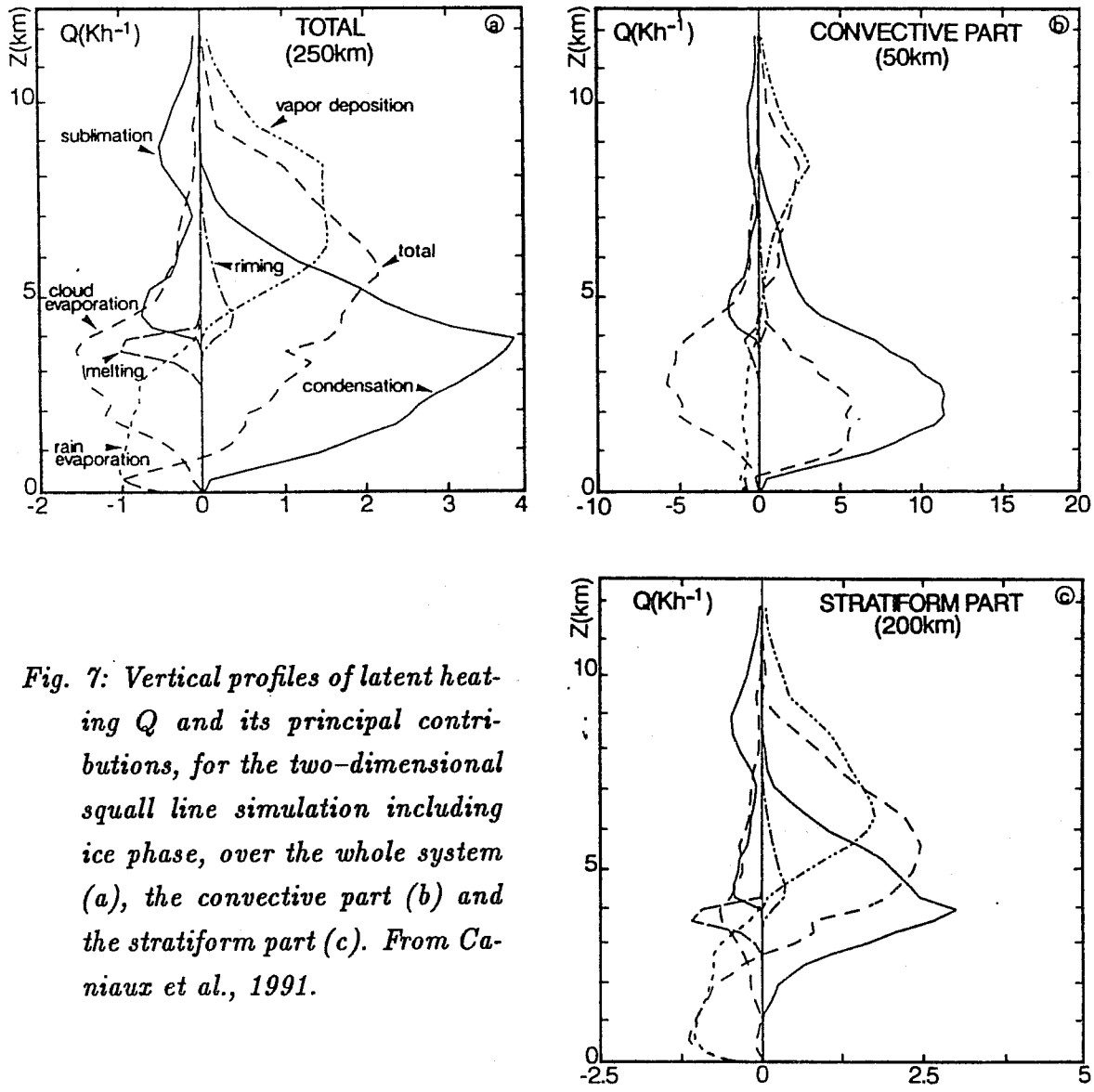

Fig. 7: Vertical profiles of latent heating Q and its principal contributions, for the two-dimensional squall line simulation including ice phase, over the whole system (a), the convective part (b) and the stratiform part (c). From Caniaux et al., 1991.

due to saturated conditions, the melting is not sufficient to produce negative values of Q as inferred by Houze (1982).

In first approximation, the profile of Q_1 follows the profile of latent heating (Fig. 8). The effect of the ice phase on the heat budget is to reduce nearly by 50 % the warming in the bright band and to increase it above by 20%. The ice phase contribution is nearly the same order of magnitude than the eddy heat transport and acts in the same way above 5 km. The ice phase contribution mainly concerns the stratiform part.

The apparent moisture sink Q_2 (Fig. 9) crudely depends on the eddy moisture transport. This result is in agreement with previous simulations of the convective part (Tao and Soong, 1986; Duhia and Moncrieff, 1987; LRJ88). It is still valid for the stratiform part and for the entire system.

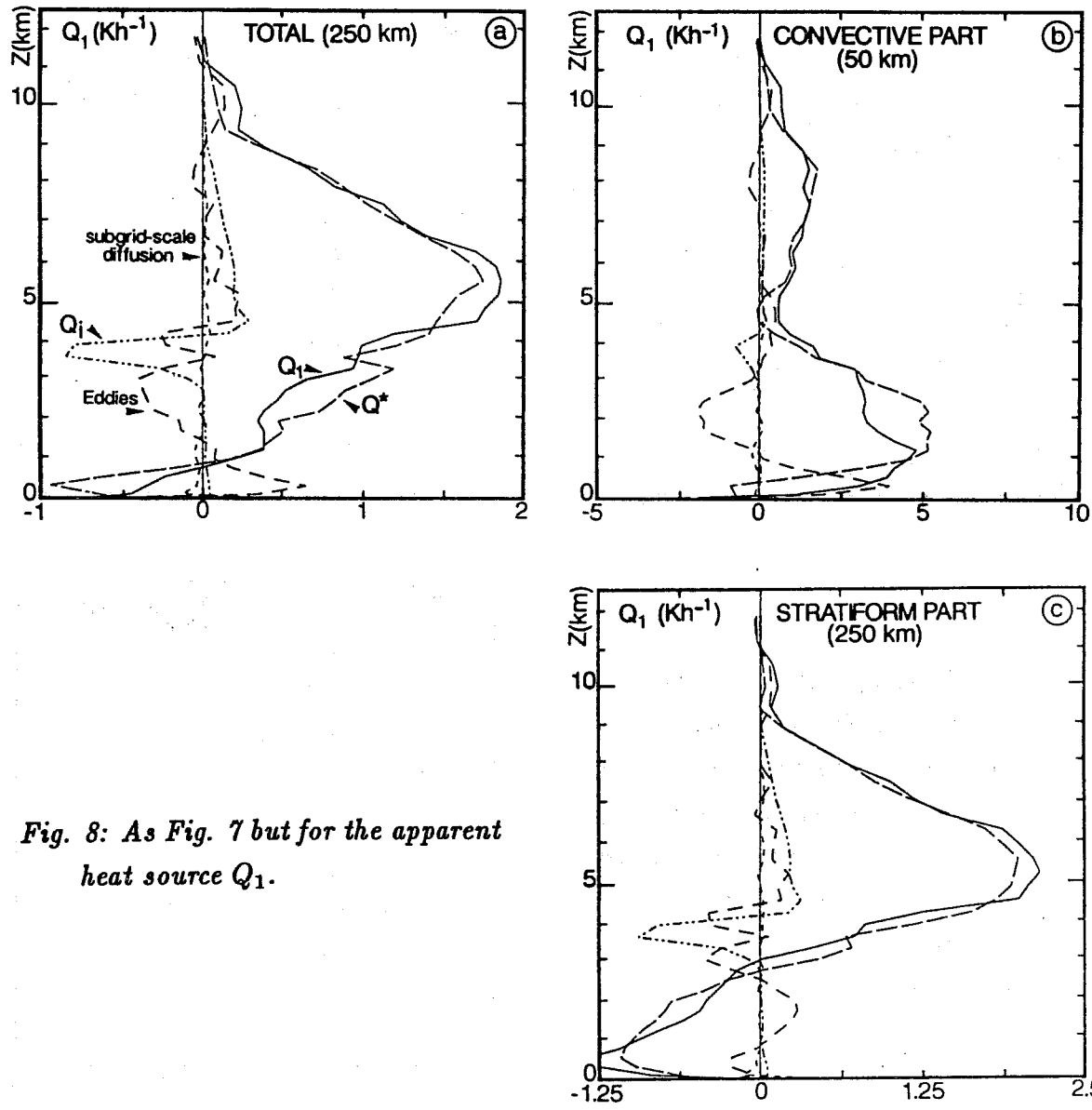

Fig. 8: As Fig. 7 but for the apparent heat source Q_1.

To compare these profiles to other simulated or observed systems, the normalization by the rainfall rate proposed by Johnson (1984) is used (Fig. 10). General form of $\hat{Q}_1$ profiles in each box is in good agreement with observed ones (Johnson, 1984; Houze, 1989; Chong and Hauser, 1990; Gallus and Johnson, 1991) (hereafter J84, H89, CH90 and GJ91). For the convective part, the simulated net cooling at low levels (Fig. 6a) was not diagnosed by J84 and H89. Recent estimations with higher resolution data by CH90 (Doppler radars) and by GH91 (rawinsondes) confirm the present numerical results for a tropical and midlatitude squall line respectively. The main difference is the altitude of the maximum of cooling in the stratiform part, much lower in our simulations (700 m) than in the previous studies. The large scale transport term added to evaporative cooling is responsible for this difference. It is not a consequence of melting as reported by Houze (1982). All studies agree on the depth of this important cooling layer, ranging

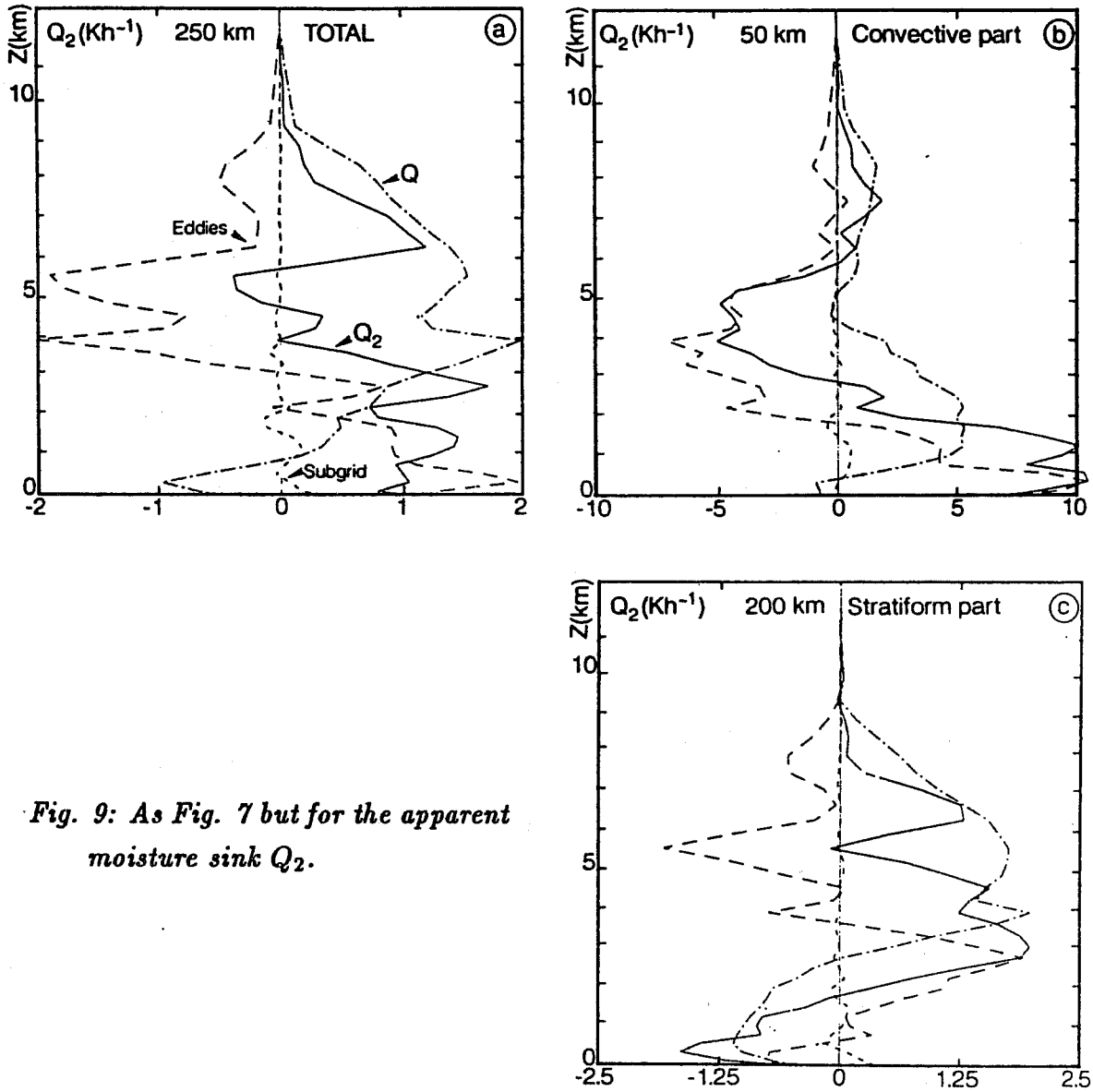

Fig. 9: As Fig. 7 but for the apparent moisture sink Q_2.

between 3 to 4 km. The altitude of the stratiform heating maximum was found is higher by GJ91, as the system dissipated.

The $\hat{Q}_2$ profile for the whole system has a similar structure to that deduced from observations by Johnson (1976) and Reed and Recker (1971). It is caracterized by a double peak structure with maxima near 3 km and 6.5 km, as already discussed. For the stratiform region, the $\hat{Q}_2^m$ budgets are less numerous than for the convective one and the present numerical results may be only compared to estimations made by Johnson and Young (1983) (hereafter JY) and CH90. The present simulated $\hat{Q}_2^m$ profile shows a moistening in low layers and drying at high levels as found by JY though lower in the present study. The maximum of simulated moistening and drying occurs at .6 km and 3 km respectively, whereas they occurring at 2 and 8 km in JY. On contrary CH90 did not diagnose a double peak structure. As discussed above, this difference is essentially due to the convective eddies transport.

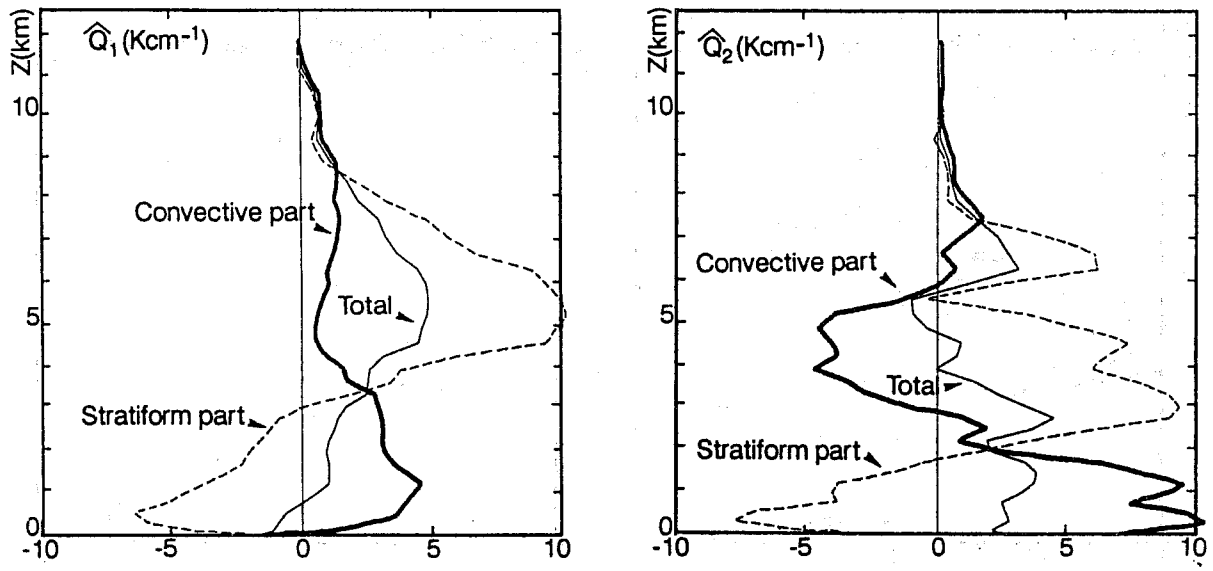

Fig. 10: Partitioning of the normalized apparent heat source (a) and moisture sink (b) into convective-scale and mesoscale components.

2.4 Horizontal momentum apparent source

Momentum transports by convection remain a difficult and poorly understood part of cloud effects on atmospheric motions at all scales. In this section, it will show that well-organized convection can transport significant horizontal momentum.

2.4.1 The formalism

As for heat and moisture it is possible to define an apparent momentum source, representing the effects of unresolved convective circulation on the mesoscale momentum field. For instance for the cross-system wind component, the apparent source of momentum is defined by:

$$Q_u = -\frac{1}{<\rho>}\langle\frac{\partial\langle\rho\rangle w'u'}{\partial z}\rangle + D_{Q_u}$$

where D_{Q_u} represents the model subgrid-scale contribution. This apparent source of momentum is easy to compute from numerical simulations in averaging in time (over 1 h) and space (over the convective and stratiform boxes). The partitioning method introduced for the Q_1, Q_2 terms will be also used.

2.4.2 Momentum vertical fluxes

LRJ88 compared simulated cross-line momentum vertical fluxes with Doppler radar observations on a 30 km width box of the convective part (Fig. 11). Although slightly stronger for observations than for simulations, the agreement is good and stresses the

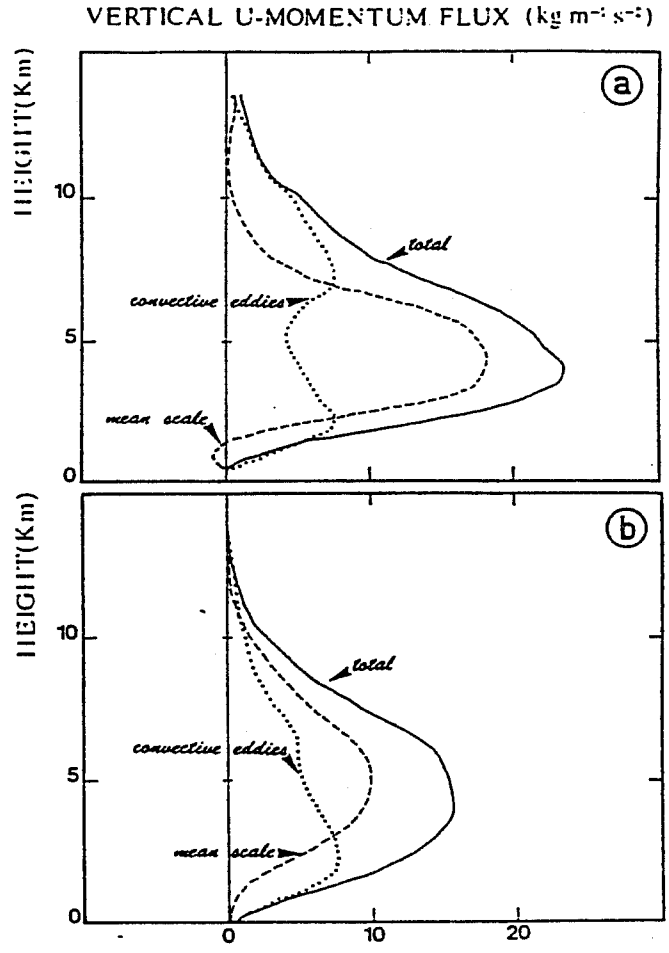

Fig. 11: Vertical line-normal u-momentum flux in the convective part of the squall line for (a) radar observations, and (b) three-dimensional simulation. (From Lafore et al., 1988)

the importance of momentum vertical transports. It is difficult to quantitatively compare these findings with previous results of LeMone *et al.*(1984), nevertheless the fast-moving lines observed during the GATE experiment show similar behaviour, as well the midlatitude squall-lines observed during the CCOPE experiment (Matejka and LeMone, 1990 ; LeMone *et al.*, 1990). As observed by Smull and Houze (1987) and LRJ88, the vertical transport of line-normal momentum in squall line is larger than the along-line one.

The momentum vertical fluxes at system scale estimated from the two-dimensional simulation (Fig. 12) bring interesting and new results. At the system scale (300 km) the total vertical transport is significant (Fig. 12a) (maximum of 0.8 kg $m^{-1}s^{-2}$ in the 2-3 km layer). Transient eddies are not negligible but the steady ones dominate. As for heat and moisture, the convective and stratiform vertical transports are different but both contribute to the total momentum vertical transport. The transport in the convective part (50 km wide) is positive (Fig 12b) and presents a maximum at 2 km

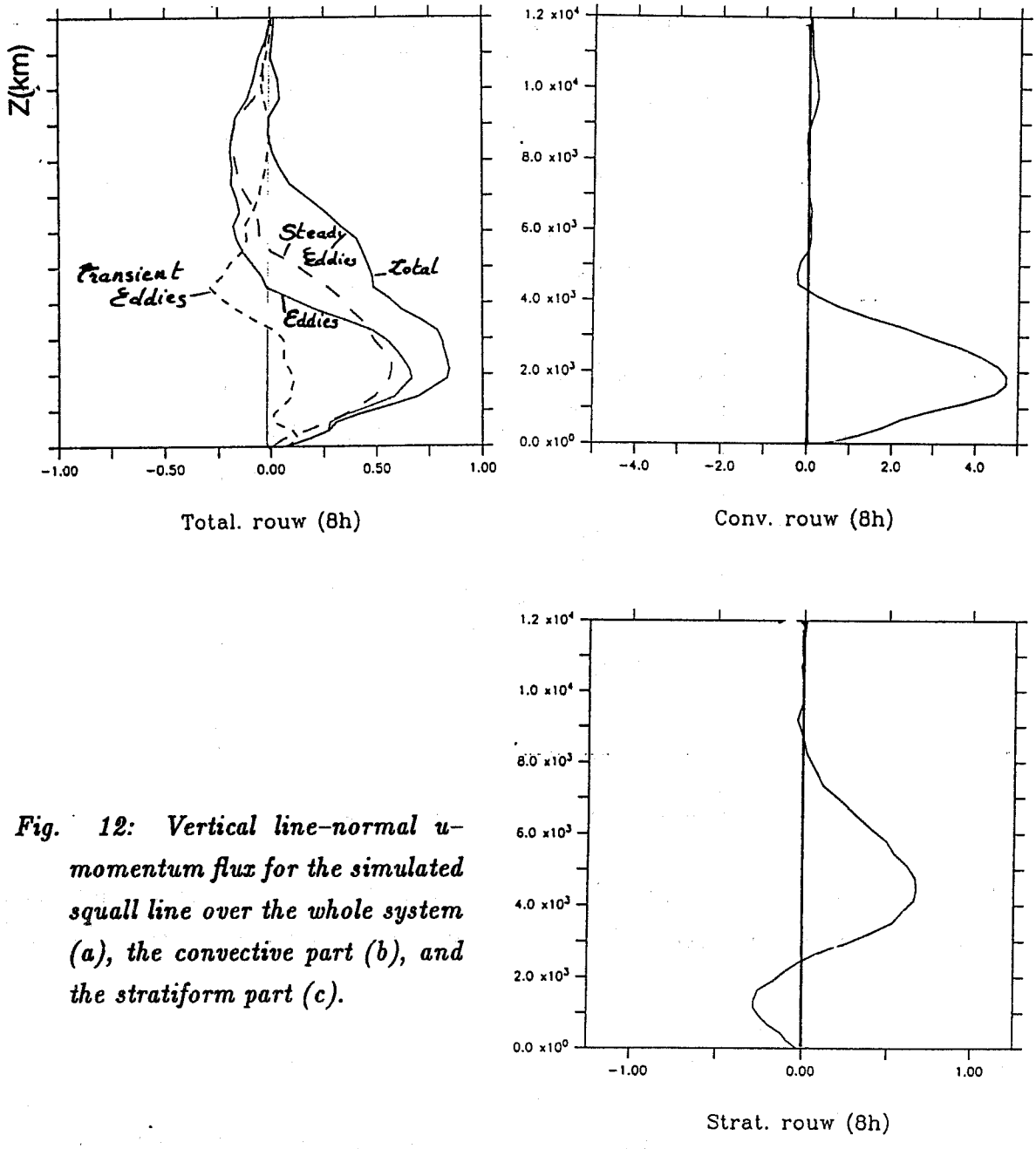

Fig. 12: Vertical line-normal u-momentum flux for the simulated squall line over the whole system (a), the convective part (b), and the stratiform part (c).

(4.8 kg $m^{-1}s^{-2}$) though underestimated due to the two-dimensional framework. The mesoscale ascent in the stratiform part (0.12 m s^{-1} over 250 km) transports momentum to the upper troposphere. The mesoscale subsidence leads to a negative momentum vertical flux below 2.5 km (Fig. 12c).

2.4.3 Apparent source of momentum

The resulting apparent source of cross-line momentum Q_u is shown on Fig. 13. Except in the PBL, the model's subgrid-scale diffusion D_{Q_u} is residual. The initial cross-line wind profile (Fig. 14) helps to figure out the impact of the convection. This wind profile is characterized by a double jet structure: the African easterly jet (AEJ)

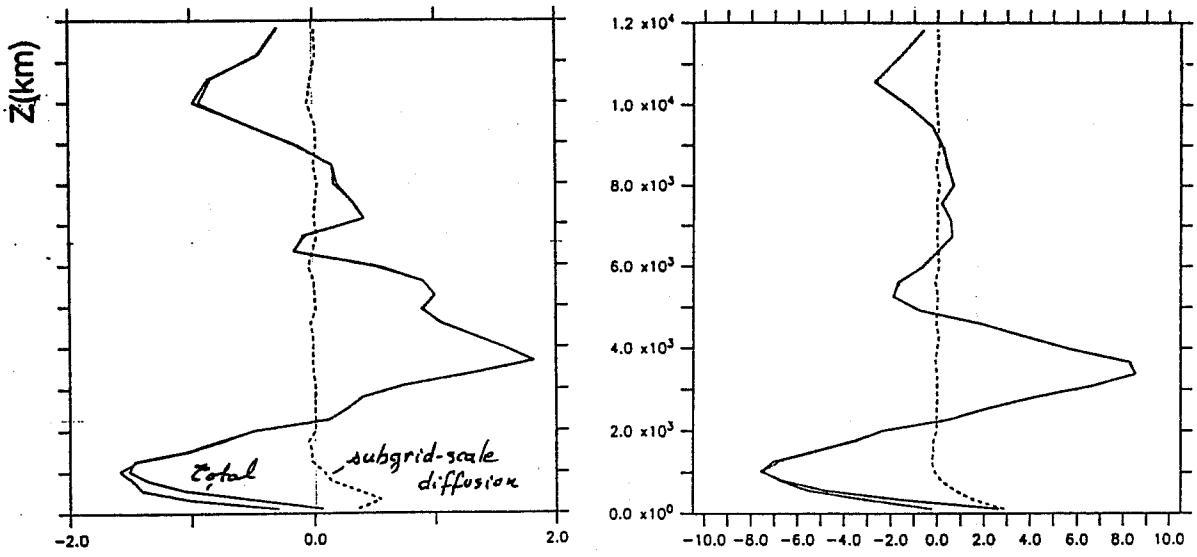

Bilan U tout domaine. (8h) (QU, VET, DIF)

Bilan U conv. (8h) (QU, VET, DIF)

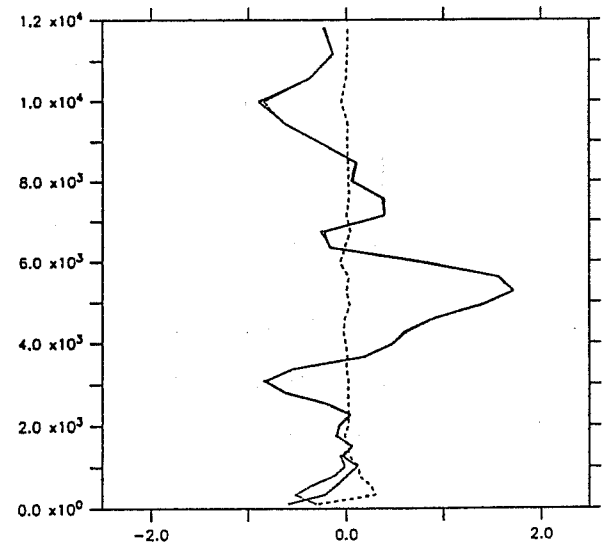

Bilan U stra. (8h) (QU, VET, DIF)

Fig. 13: As Fig. 7 but for the apparent source of line-normal u-momentum Q_u.

and the Tropical easterly jet (TEJ) at levels 14 km and 3.5 km, respectively. The AEJ height also corresponds to an intense θ_e minimum ($\Delta\theta_e = -29°$ relative to the θ_e sub-cloud value) and results in an intense shear at low levels ($\Delta U \simeq 15ms^{-1}$ over 3.5 km).

The effects of the whole system (Figs. 13a) are a deceleration below 2.3 km (maximum of - 1.5 m s^{-1}/hour), an acceleration up to 8.7 km (maximum of 1.8 m s^{-1}/hour at the AEJ height) and a deceleration above (maximum of -1 m s^{-1}/hour at 10 km). It means that the SL significantly decreases the low level shear and the AEJ intensity, mainly due to the convective part (Fig. 14b). The rear to front acceleration (1 m s^{-1}/hour at 3 km) in the stratiform part, prevents in part the AEJ weakening, due to the induced pressure horizontal gradient at the base of trailing anvil (Lafore and Moncrieff, 1989). Above 4 km, the front to rear acceleration is due to the stratiform part.

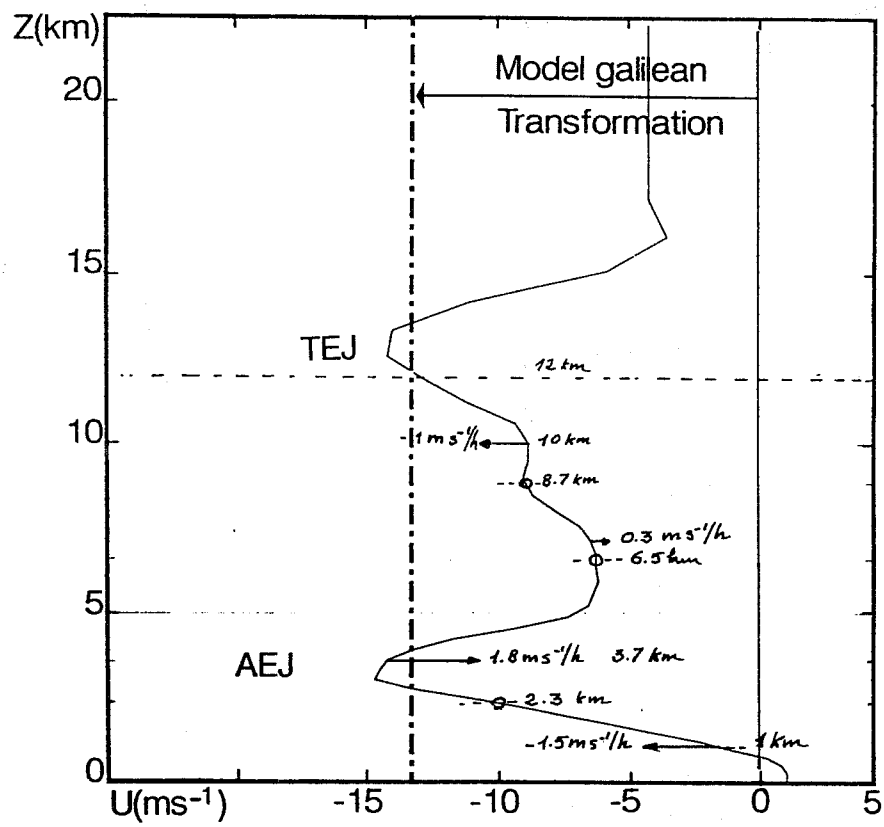

Fig. 14: Initial cross-line wind profile for the squall line simulation. The arrows are proportional to the apparent momentum source intensity, and allow to figure out the dynamical effect of the convection at the system scale.

Above 10 km just below the TEJ, both stratiform and convective parts develop a rear to front acceleration, resulting the intensification of the forward anvil. This typical meso-β-scale wind perturbation induced by the system was also observed by Chalon *et al.*(1988) for the 23 June squall line case, and simulated by Lafore and Moncrieff (1989).

The main results of this analysis are that momentum vertical transport is not negligible at large-scale and that the stratiform part contribution can be significant in some case.

2.5 Discussion on the squall line case

Although the present goal is not to explain our physical understanding of the organized convection, it is useful to know the environment conditions which are favourable for its development. Observations (Barnes and Sieckman, 1984), theoritical and numerical studies (Moncrieff, 1981; Rotunno et al., 1988; Moncrieff and So, 1989; Lafore and Moncrieff, 1989 among others) suggest that three environmental parameters are recognized to control the growth, evolution and organization of SL. It sounds good to propose them as the basic physical parameters to develop convection parameterization schemes. These three parameters are the convective available potential energy (CAPE), the wind shear or shift ΔU, between the PBL and the middle layer air, and the potential instability of this last dry layer (low θ_e) to downward displacement (SAPE for subsident). The last parameter is not pointed out by all studies and is difficult to quantify. However, this quantity seems to play a major role in the formation of the density current helping to organize such systems.

The previous budget calculations show that the system activity induces modifications of the environment. It results in a decreasing of the CAPE and SAPE values, mainly at the system rear for fast moving squall lines. Considering that the inflow conditions are weakly modified, that explains why such system can reach a long lasting stage. The last basic ingredient ΔU is also affected by the system activity. For instance in our simulations, the shear decreases up to 3 to 4 m s^{-1}/hour over a 4 km layer, that may desorganize the system itself. That suggests the needing of a more physically treatment of all effects of organized convection on thermodynamic and momentum fields.

Although the interaction between the convective and stratiform part are now better understood, the effect of momentum vertical transport at larger-scale is poorly understood and documented. Further works are needed to establish the relationship between the large-scale flow and the resulting fluxes, with the help of analytical theories such as the non linear one established by Moncrieff (1981) for steady state regimes of organized convection in shear environment.

3. THE FRONTAL SYSTEM CASE

One specific scientific objective of the MFDP/FRONTS87 project was to obtain an improved dynamical understanding of synoptic, meso and smaller scale interactions in active cold fronts. As a major part of the french contribution, the french nonhydrostatic cloud model (Redelsperger and Sommeria, 1986) has been used to perform two-dimensional high resolution simulations of the IOP 2 case.

Before to simulate FRONTS87 cases, a series of numerical experiments with high resolution (5km) have been performed with an analytical solution to the Eady problem (Hoskins and Bretherton, 1972) as initial condition (Benard *et al.*, 1991 a and b). These experiments have shown the ability of models working at cloud scale to reproduce most of mesoscale features, generally observed in the frontal systems. Namely, the large variety of rainbands observed by radars were simulated (Fig. 15 a).

To simulate the IOP2 case with the nonhydrostatic cloud model (horizontal resolution of 5 or 20 km here), the French forecast hydrostatic "Péridot" model (horizontal resolution of 35 km) has been used to provide the initial fields. The "Péridot" fields are also used to monitor the large-scale forcing through an one-way coupling between the two models.

The mean cross-front structure at 18 h on the 11 September 1987, is computed from the "Péridot" fields. A stationary state is assumed to describe the large-scale forcing through shear and deformation in the system moving-frame (11 m s^{-1} and 15 m s^{-1} in the cross and along-front directions respectively). The figures 16b and 16c show the velocity field on an inner region of the domain for simulation using horizontal resolutions of 5 and 20 km respectively. Many features observed in the previous simulations of Eady problem (Fig. 15 a) are also found in the 5 km resolution experiment (Fig. 15 b). Two classes of narrow bands are identified: A Narrow Cold–Frontal Rainband at the surface cold front and Narrow Free–Atmosphere Rainbands (NCFR and NFAR respectively, hereafter). Two classes of wide bands are also observed: Wide Cold–Frontal Rainbands and Warm Sector Wide Rainbands (WCFR and WSWR respectively, hereafter).

3.1 Comparisons with observations

The simulation of POI2 case needs around 3 h to reach a nearly steady state (Fig. 16 a) comparable with Doppler radar observations (Fig. 16 b) performed in the VAD mode (Jaubert *et al.*, 1991), as the cold front reached the french coast. Wavelengths shorter than 40 km has been removed to the simulation fields (Fig. 16 a,c) to be able to compare with observations. In explicitly simulating both convection and large-scale flow, the model is able to reproduce observed circulation and the large variety of rainbands. It is not the case with the 20 km non–hydrostatic simulation as well with the Péridot hydrostatic simulation. The along-front low level jet is also closer to observations (Fig. 16 c,d) with a better position than for Péridot simulations. Some preliminary results of a Péridot simulation using a modified parameterization of the convection including the downdrafts effects, confirm the importance of diabatic processes to reproduce the observed structure of front in the low troposphere.

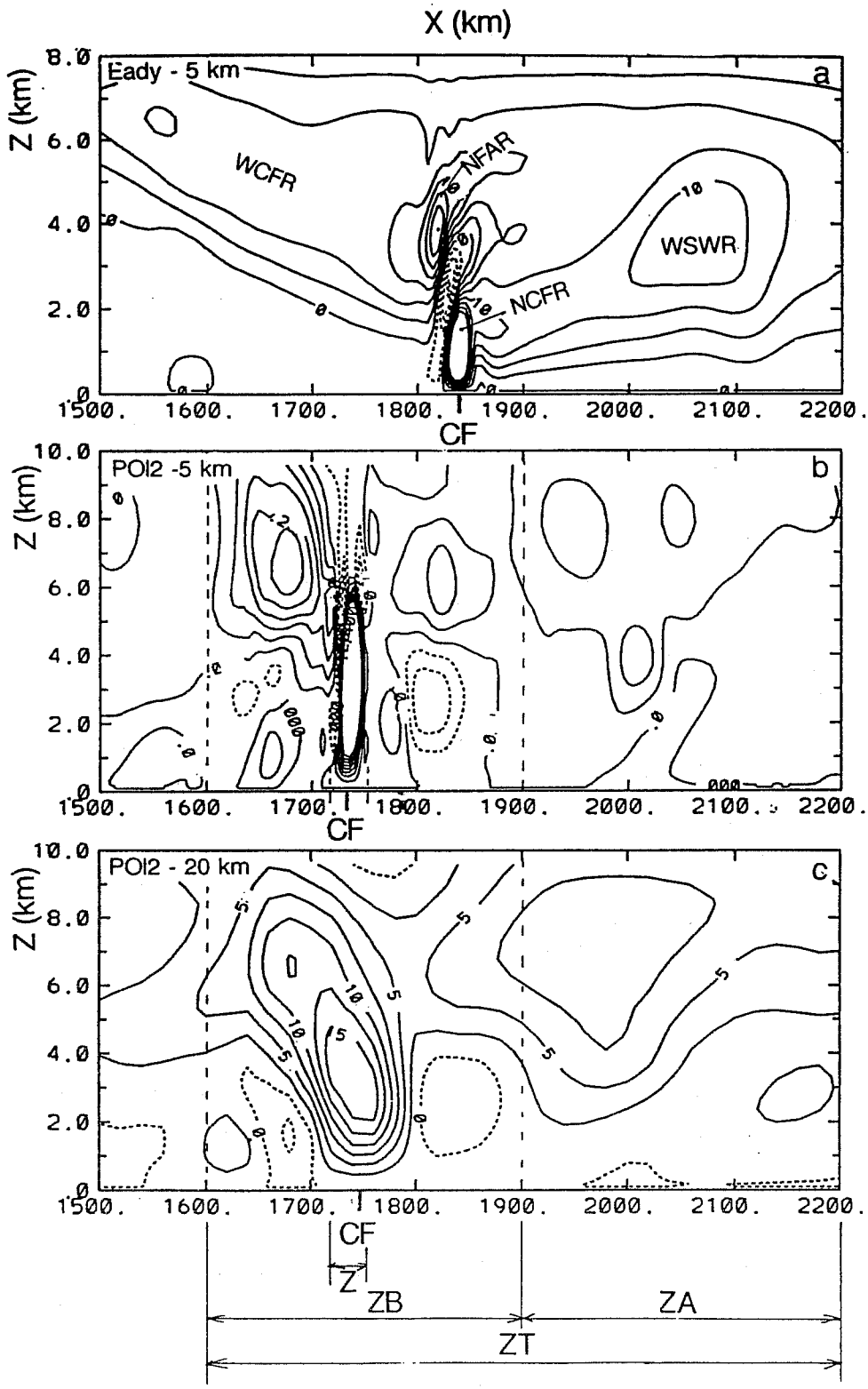

Fig. 15: Cross sections of vertical velocity, for simulation of the moist Eady problem (a) with 5 km horizontal resolution (contour interval 2.5 cm s^{-1}), and for the Fronts87 simulation with 5km (b) and 20 km (c) horizontal resolution (contour interval 5 cm s^{-1}).

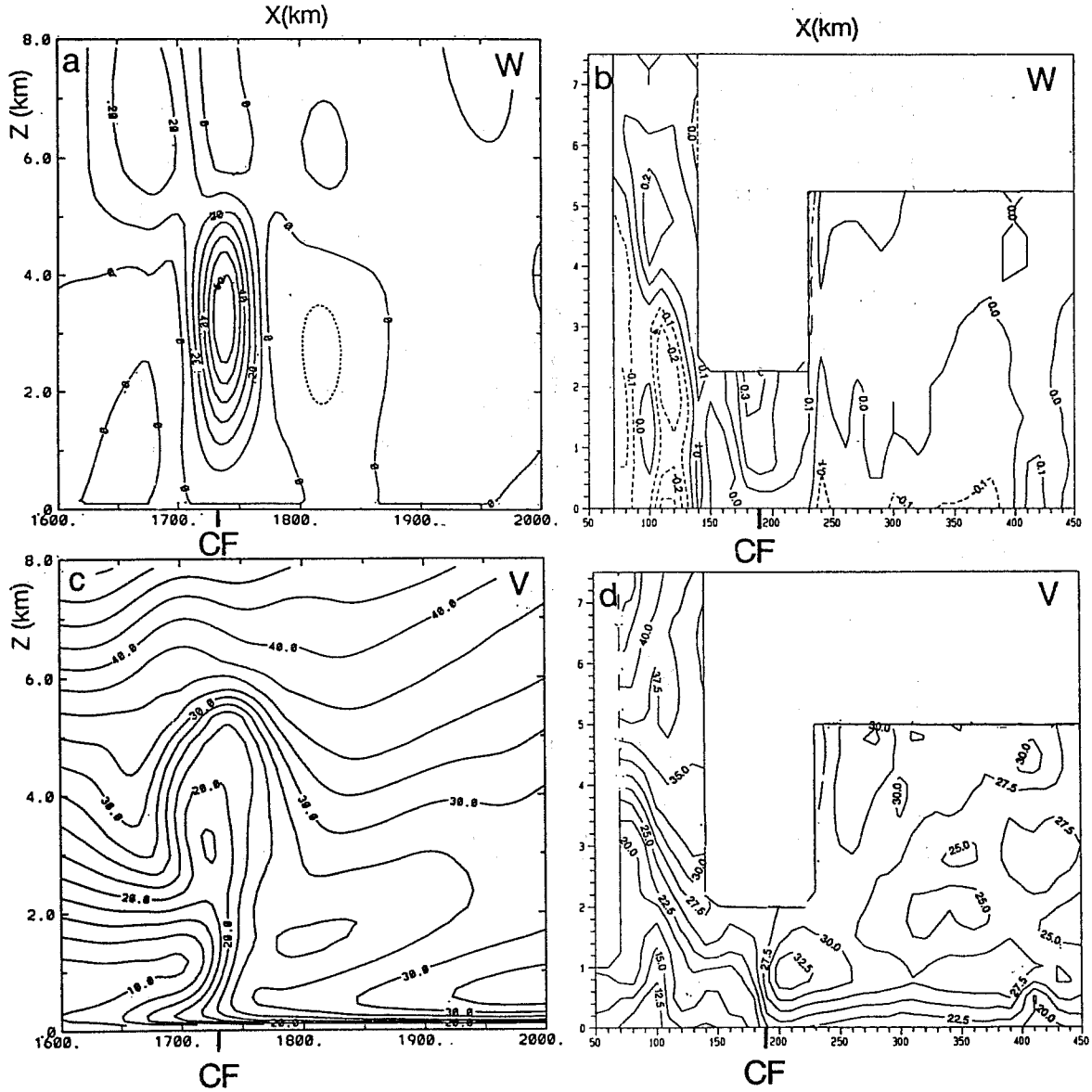

Fig. 16: Comparisons between simulation and Doppler radar observations for the vertical velocity (a and b) (contour interval .1 m s^{-1}) and along-front wind (c and d) (contour interval 2.5 m s^{-1}) fields. The model fields are filtered (40 km wavelength cut-off) in order to match with the radar resolution.

The simulated and observed precipitation patterns at the ground are compared on Fig. 17. The rain gauges data are time and space averaged on a 15 mm - 50 km scale, whereas simulated precipitation rates are presented at the model resolution (5 km). Accounting of these differences, the NCFR is well marked with maximum values in agreement with local maximum at each station. Also the wide spread precipitation in the (WSWR) is found. On contrary the WCFR does not produce significant rain at the ground. The total mean precipitation over the 400 km width of the system (1.5 mm h^{-1}) is close to observations. Note that the simulations with a cruder resolution of 20 km produce less precipitation ($\sim$ 1 mm h^{-1}).

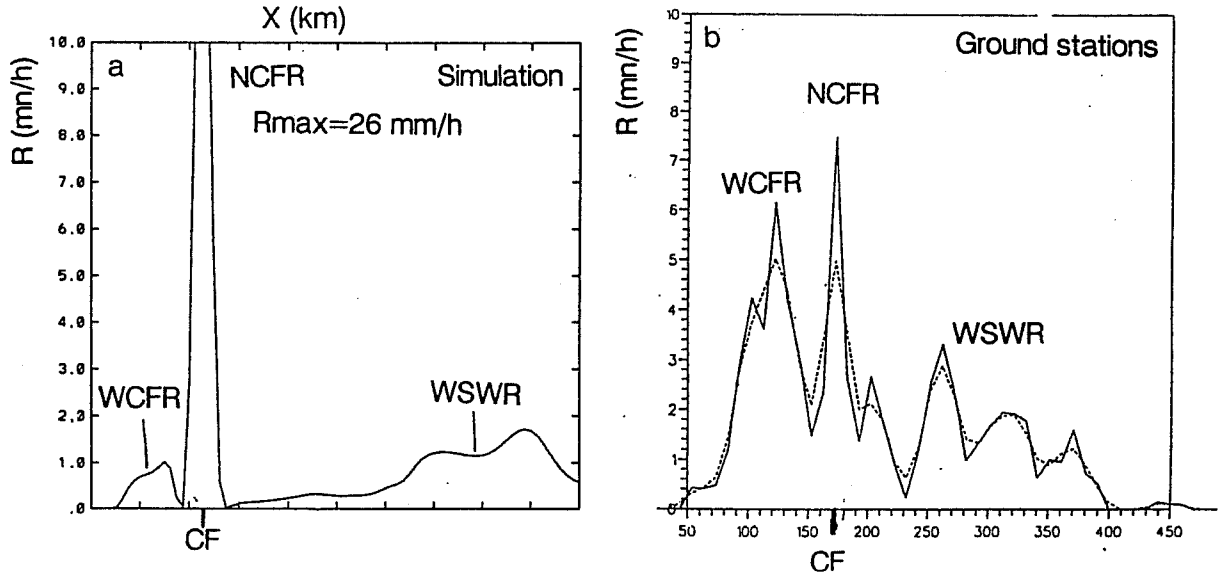

Fig. 17: Comparisons between simulated (a) and observed (b) precipitation rates at the ground. Rain gauges data are space and time averaged on a 50 km – 15 mn scale, whereas simulated fields are instantaneous and at 5 km resolution.

3.2 Heat and moisture budget

Most of results presented in this subsection will focus on the 5 km simulation of the POI2 case. The same formalism developed for squall lines in the previous section 2 will be used, except that the solid phase contribution is null as the ice parameterization has not been included in the present numerical experiments. Four zones have been chosen to present the budget calculations (Fig. 15). The zone labelled ZT covers the frontal system for its most intense part (600 km wide). We subdivided it in 2 sub-regions ZA and ZB (300 km wide), surrounding the cold front and in the warm sector respectively. The γ–scale region Z (30 km wide) documents the NCFR activity.

3.2.1 Latent heating

The different contributions to the latent heating Q for the main part of the frontal system are shown on Fig. 18 a. The net latent heating indicates a global warming due to condensation through the troposphere, except in the first km where rain evaporation leads to a cooling of .8 K / h. The analysis of these profiles in the different sub-regions Z, ZA and ZB (Fig 18b,c,d) allows to draw following conclusions:

– The NCFR represents the principal contribution (Fig. 18 b) to the total heating by condensation at low levels (0 to 3 km).

– The wide bands WCFR and WSWR (Fig 18c and d) mainly contribute to heat the middle and upper troposphere.

– The intense cooling by rain evaporation mainly results from the trailing precipitation of wide bands , and occurs up to altitude of 4.5 km in the cold frontal zone.

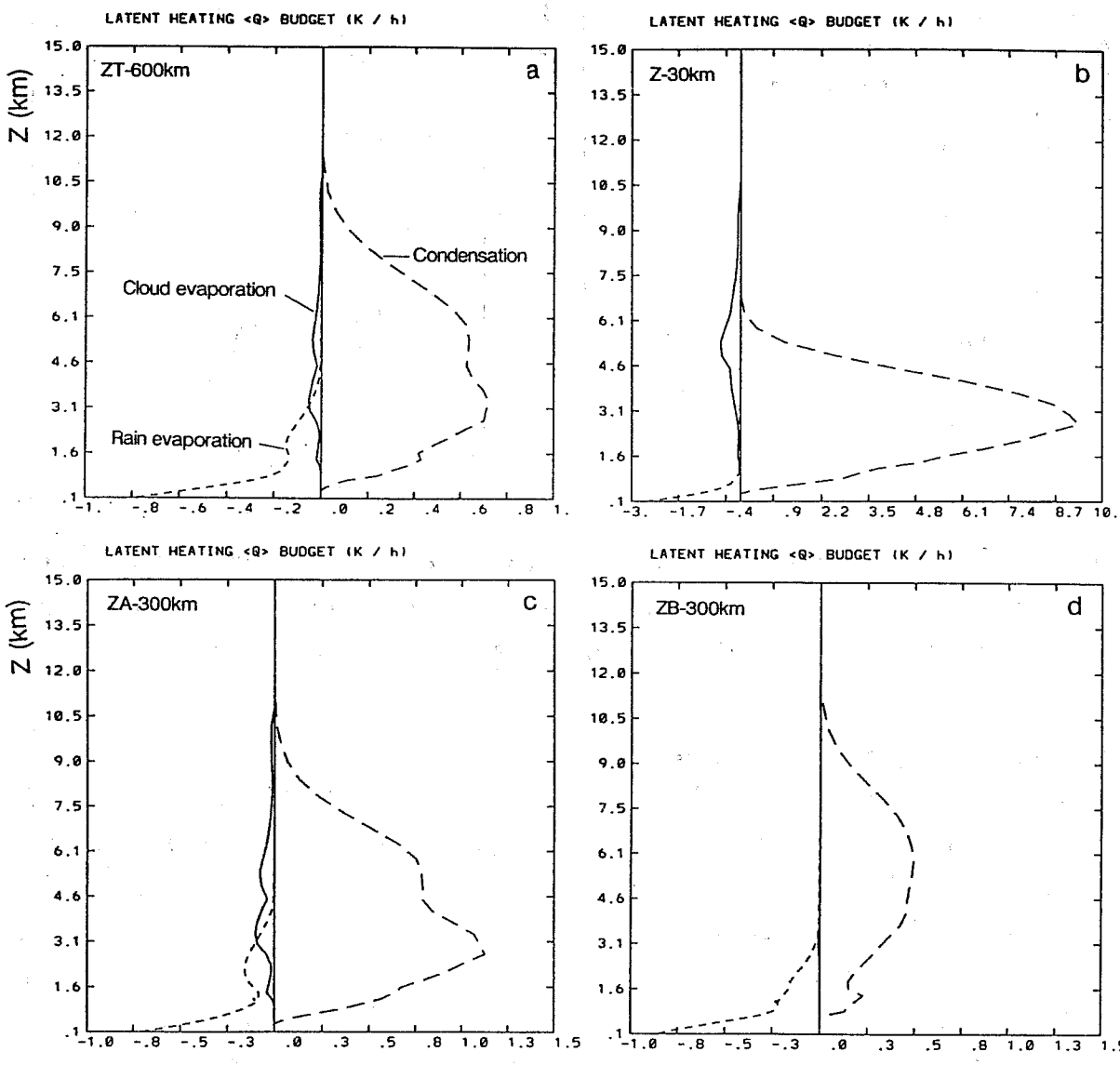

Fig. 18: Vertical profiles of latent heating for the Fronts87 simulation with 5 km resolution, for the ZT, Z, ZA and ZB zones (see text and Fig. 15.

3.2.2 Heat and moisture apparent sources

The vertical transport of heat and especially moisture by the NCFR (Fig. 19b and 21b) is important and is still seen at the system scale (Fig. 19a and 20a) in the heat and moisture apparent sources through the eddies term. On contrary the contribution

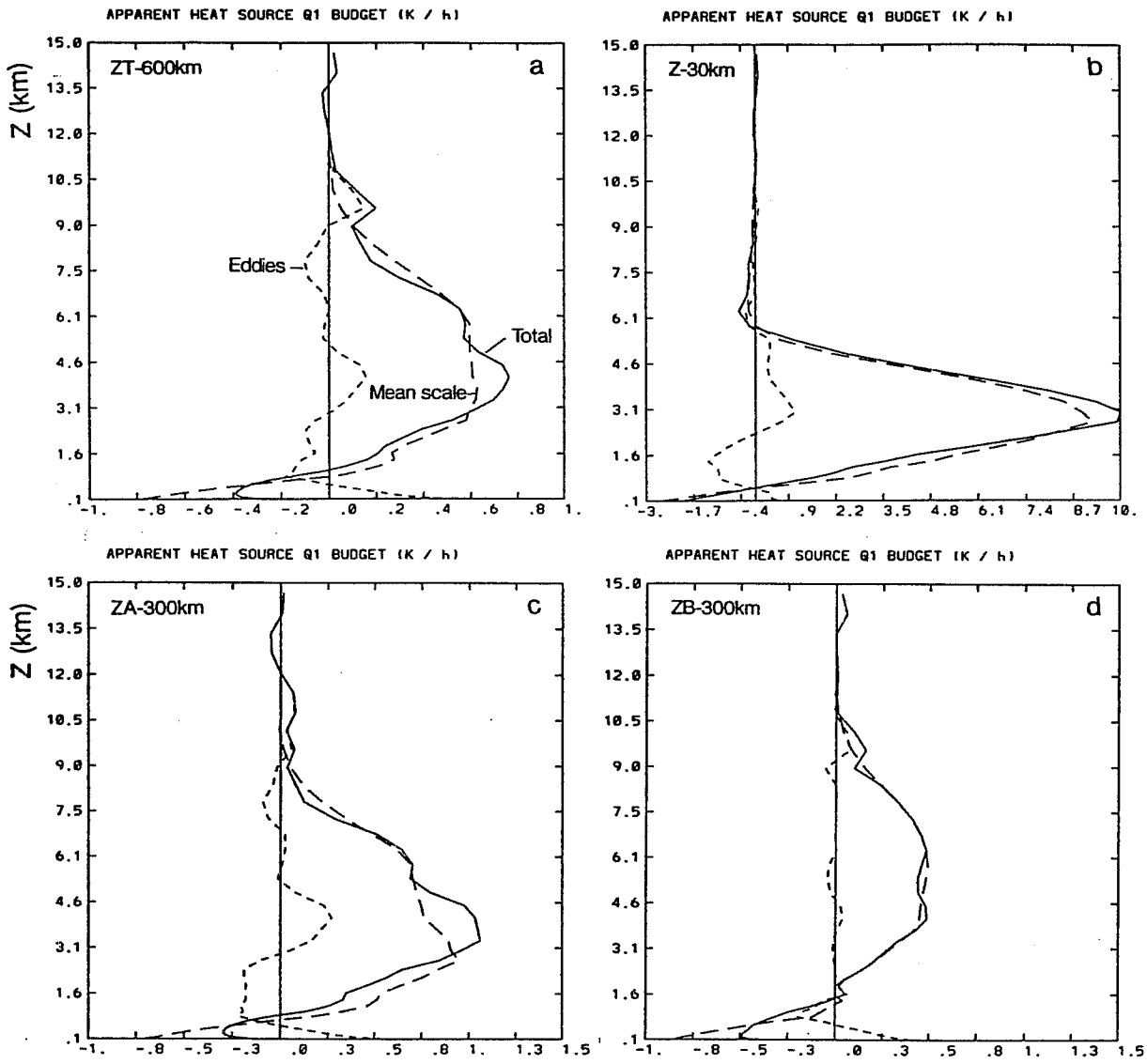

Fig. 19: As Fig. 18 but for the apparent heat source Q_1.

of wide bands to the eddies term is weak. In the planetary boundary layer (PBL) and in every region of the system, the eddies terms are important and decrease the total effect. That stresses the importance of a good representation of the PBL, that should be coupled with the convection parameterization scheme in GCM.

Therefore the parameterization of the transports occurring in the NCFR, must be included in the eddies term. As found for the squall line case, the eddies transport becomes important for the Q_2 profile, which is not well approximated by the latent heating profile Q. Also the double–peak structure of Q_2 profile due to the NCFR activity is important in the ZA zone (Fig. 20c), and is still present at the system scale ZT (Fig. 20a).

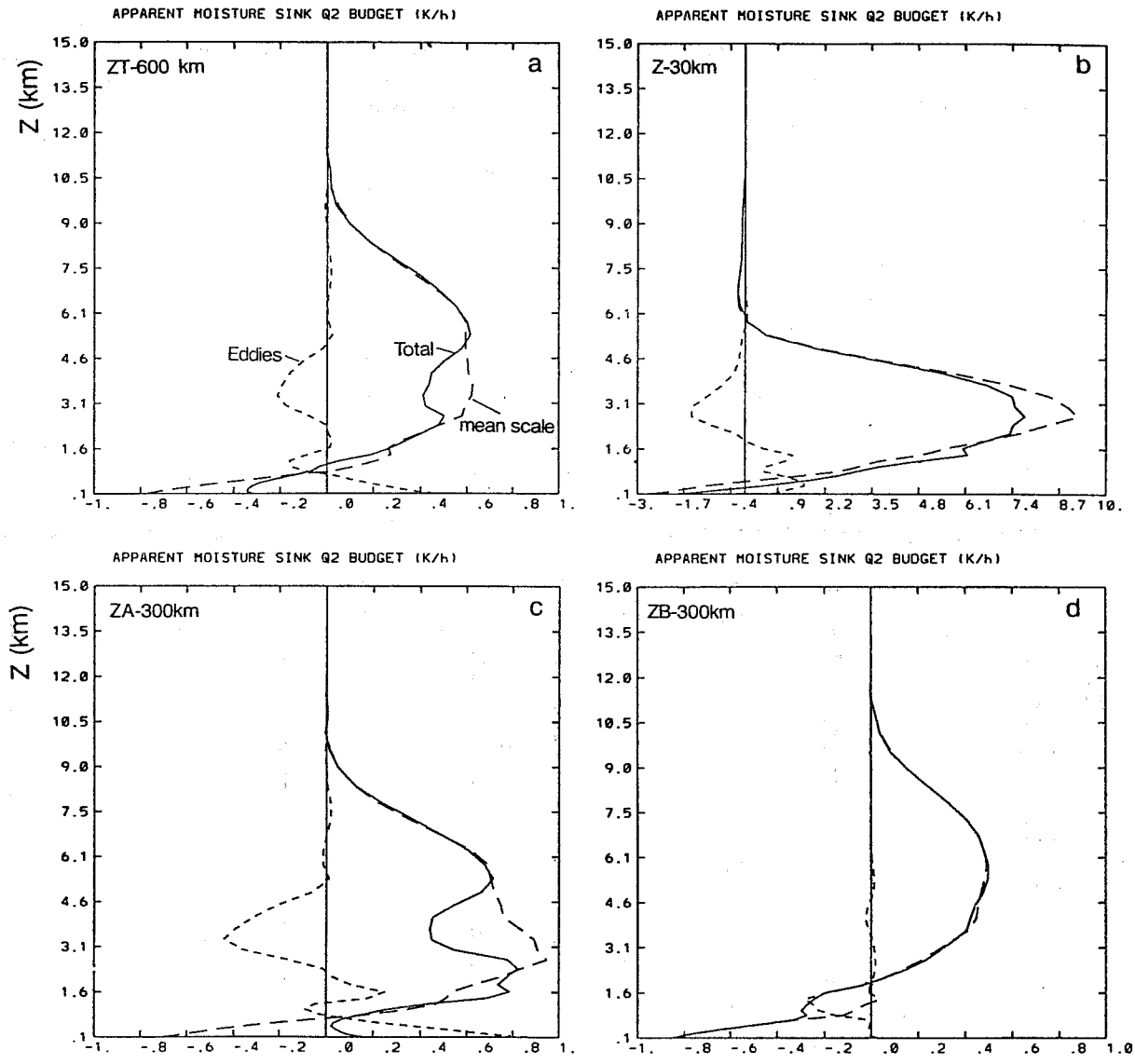

Fig. 20: As Fig. 18 but for the apparent moisture sink Q_2.

3.2.3 Normalized heat and moisture apparent source

Figures 21a and b show heat and moisture apparent source normalized by the rainfall rate as made for squall lines in section 2.3. Some similarities with tropical cases are striking. The NCFR effects (Z in Fig. 21) look like the effects of the squall line convective part (Fig. 6), but occur on a shallower depth (5 km). The main difference consists in the absence of double peak structure for the $\hat{Q}_2$ profile at this scale. The wide bands profiles (ZA and ZB in Figs. 21) look like the squall line stratiform part ones (Figs 10), with intense cooling/moistening occurring in the low troposphere, and heating/drying above. Nevertheless at the system scale the similarities are weaker, since the low levels cooling/moistening net effect by wide bands dominate contrary to the tropical cases. Also the double peak $\hat{Q}_2$ structure is weaker for the frontal cases and more related to the difference of altitude of narrow and wide band activity.

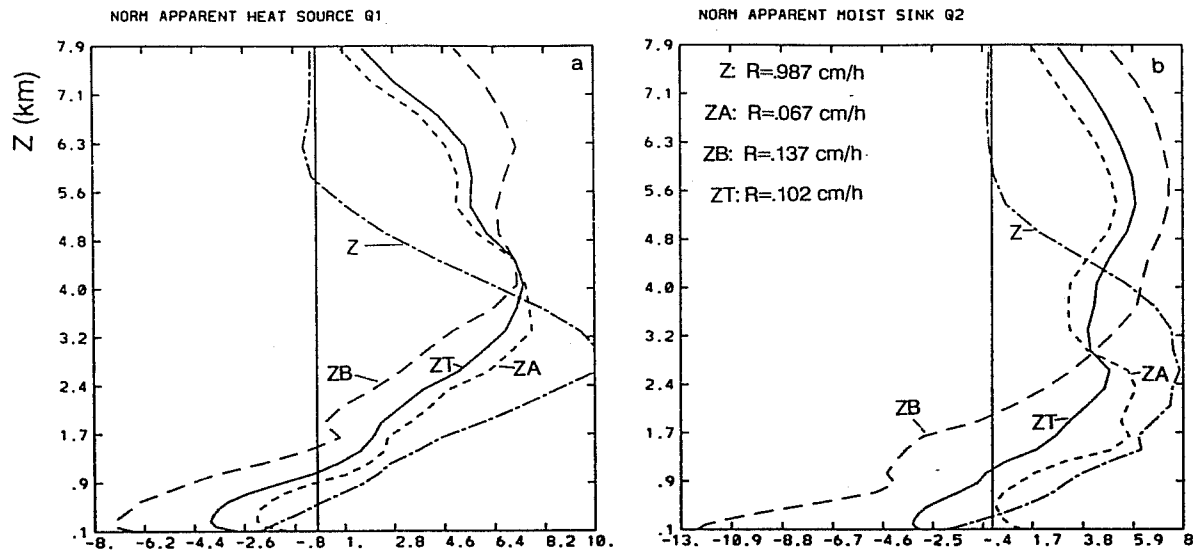

Fig. 21: Vertical profiles of normalized apparent heat source $\hat{Q}_1$ (a), and of normalized apparent moisture sink $\hat{Q}_2$ (b), for the Fronts87 simulation with 5 km resolution, and for the ZT, Z, ZA and ZB zones.

At present time the absence of similar profiles deduced from observations, avoids a necessary comparison of simulations with the reality. Recent three–dimensional doppler radar analysis performed in the NCFR (Chong *et al.*, 1991) could be used to estimate such profiles and validate the present results. The three–dimensional nature of the system in the NCFR may slightly modify the present results.

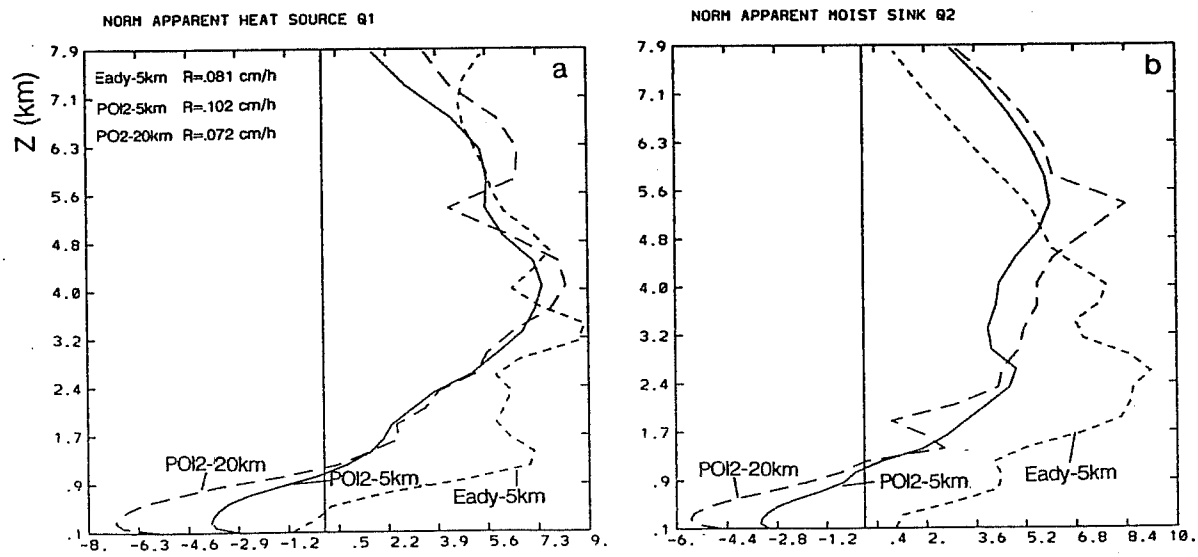

Fig. 22: Vertical profiles of normalized apparent heat source $\hat{Q}_1$ (a), and of normalized apparent moisture sink $\hat{Q}_2$ (b), over the whole system scale for three simulations: the moist Eady problem with 5 km horizontal resolution, and the Fronts87 case with 5 km and 20 km resolutions.

The $\hat{Q}_1$ and $\hat{Q}_2$ normalized profiles computed from other simulations (Figs 22), bring some interesting results. The cooling/moistening effect in low troposphere, is not obtained for the simulation of the Eady problem, due to different humidity conditions. It illustrates the variability that is expected in the nature. The horizontal resolution has a dramatic effect on the amount of cooling/moistening occurring at low levels. As viewed before, the 20 km resolution simulation produces 30 % less precipitation than the 5 km one. That induces almost a doubling of the normalized cooling/moistening rate.

3.3 Horizontal momentum apparent sources

The analysis of the horizontal momentum vertical transports and apparent sources, allows to consider 3 different regions. In the PBL the friction at the ground, induces intense momentum transports and sources. Benard *et al.* (1991b) analyzed in details the frontal PBL structure for the simulation of the Eady problem. Based on a budget of the moist potential vorticity, they demonstrated the role of friction to structure the PBL, and modify the frontal ageostrophic circulation. In the free atmosphere the momentum transports and sources are negligible, except in the NCFR. In the present stage of the analysis no clear organization of these transports have been identified for the NCFR in our simulations. Work is needed to further understand the momentum transport in the NCFR, where three–dimensional effect should be considered. Nevertheless except in the PBL, the momentum transports appear less crucial in frontal systems than for well organized tropical convective systems

4. CONCLUSION and RECOMMENDATIONS

In this paper we first tried to demonstrate the ability of fine-scale models to realistically simulate convective systems, as observed during field experiments. An important consequence of this agreement between observations and simulations, is the possibility of use simulation results to perform budget of various parameters in order to develop or test convection parameterisation.

We illustrated this approach on two very different flow regimes. A fast-moving tropical squall-line of the COPT81 experiment, represents an extreme case of well-organized unbalanced MCS. The strongly balanced flow case, has been illustrated by a frontal system observed during the European MFDP/FRONTS87 experiment. Water heat moisture and momentum budgets and vertical transports have been presented to discuss the effects of convection at larger scales for these two types of cloud systems. Beside numerous results obtained, it is interesting to attempt a comparison between two type of flow regimes. The main similarity is that the NCFR effects look like the

effects of the squall line convective part, whereas effects of wide frontal bands look like squall line stratiform parts.

The first type of organisation (NCFR and convective part) occurs on the γ–scale and is strongly three–dimensional. The heating profiles are intense and similar except on a shallow layer for NCFRs, and represent a major contribution to the whole system. Nevertheless their origins are quite different, as the convective part is convectively driven (positive CAPE), whereas NCFR is more dynamically forced. It is a major difference leading to different formulation in the frame of the analytical theory of Moncrieff (1981).

The typical structure of the Q, Q_1 and Q_2 profiles for wide frontal bands and stratiform parts of squall lines, shows a cooling/moistening at low levels and a heating/drying above. The depth of the low level layer of cooling/moistening seems deeper for squall lines than for the frontal case (2-3 km versus 1 km). Rain evaporation associated with light precipitation in these wide spread regions, is efficient to produce this layer in both types of system. It confirms the conclusion of Thorpe and Clough (1991) on the importance of evaporation in frontal systems of Fronts87, as suggested by the analysis of dropsondes. It is also in agreement with the better results of Péridot model, when using a convection parameterisation scheme including the downdrafts effects, to simulate squall line and frontal system. The effect of ice phase at large scale has been tested for the squall line case. It is not negligible in the stratiform part melting layer and above (20 %). Similar impact are expected for wide frontal bands.

The total large scale effect of convection is different for the two types of system. In the frontal case, most of effects result from the wide bands, except in the low troposphere. In the squall line case, the effects due to the convective part are larger than the ones due to the stratiform part one, except during the dissipating stage of the squall line. Another difference consists in the extreme importance of turbulent vertical transports occurring in the frontal PBL, compared to the squall line case.

Due to the importance of moisture vertical transport by convective eddies, the apparent moisture sink is very different from the Q and Q_1 profiles. The double peak structure is obtained for both systems, but with a stronger signature for the squall line case. Parameterisation schemes should include a representation of the moisture vertical transport by convective eddies.

The horizontal momentum transport is intense for fast-moving squall-lines both in convective and stratiform parts. For instance the resulting cross-line momentum apparent source can reach 1 to 2 m s^{-1}/hour over 300 km. This dynamical effect should be taken into account at larger scale and can help to diagnose the dissipating stage of the MCS. Momentum transport appears less crucial in frontal systems than

for well organized MCSs, except in the PBL and in the NCFR region.

This paper allows to propose some recommendations.

• Fine-scale modelling studies should be extensively used to performed budget analysis of heat moisture and momentum, in order to help to the development or tests of parameterisation schemes. Collaboration between fine-scale modelers and experts in parameterisation must be encouraged and organized.

• An important step is to compare these simulations with observations, to validate them and estimate their limits. The need of appropriate field experiments has to be stressed (TOGA/COARE).

• The realism of fine-scale simulations must be improved at least on three points: the initialisation procedure, the treatment of the interaction between the convective system and the large scale flow, and the increase of the number of three–dimensional simulations.

• The complete life cycle of organized convective systems is poorly documented and understood. Studies of the convection initiation and dissipation stages should be encouraged.

• Parameterisation schemes should include in priority the rain evaporation and the moisture vertical transport by convective eddies. Particular attention must be put on the dryness of the middle troposphere and on a good representation of the PBL, that should be coupled with the convection scheme.

• Further studies are needed to better understand the dynamical transport by convection, to find a consistent unified way to parameterize all together the heat, moisture and momentum large scale effects, especially for well organized convective systems.

5. REFERENCES

Barnes, G.M., and K. Sieckman, 1984: The environment of fast– and slow–moving tropical mesoscale convective cloud lines. *Mon. Wea. Rev.*, **112**, 1782–1794.

Bénard, P. , J.L. Redelsperger, and J. P. Lafore, 1991a: Non–hydrostatic simulations of frontogenesis in a moist atmosphere. Part I: general description and narrow frontal rainbands. Submitted to *J. Atmos. Sci.*.

Bénard, P., J.–P. Lafore and J.–L. Redelsperger, 1991b: Non–hydrostatic simulation of frontogenesis in a moist atmosphere. Part II : Moist potential vorticity budget and wide rainbands. Submit to *J. Atmos. Sci.*.

Browning, K. A., Hoskins B.J., Jonas P.R., and Thorpe A.J., 1986: European collaboration on atmospheric fronts. *Nature*, **322**, 114–115.

Caniaux, G., J.–L. Redelsperger, and J.–P. Lafore, 1991: A numerical study of the stratiform region of a fast–moving squall line. Part I: General description, and water and heat budgets. To submit to *J. Atmos. Sci.*.

Caniaux, G., J.–P. Lafore, and J.–L. Redelsperger, 1991: A numerical study of the stratiform region of a fast–moving squall line. part II: Relationship between mass, pressure and momentum fields, and momentum budgets. To submit to *J. Atmos. Sci.*.

Chalon,J.P., G.Jaubert, F. Roux, and J.P. Lafore, 1988: The West African squall line observed on 23 June 1981 during COPT81: Mesoscale structure and transports. *J.Atmos.Sci.*,**45**,2744-2763.

Chong, M., and D. Hauser, 1989: A tropical squall line observed during the COPT 81 experiment in West Africa. Part II: Water budget. *Mon. Wea. Rev.*, **117**, 728-744.

Chong, M., and D. Hauser, 1990: A tropical squall line observed during the COPT 81 experiment in West Africa. Part III: Heat and moisture budgets. *Mon. Wea. Rev.*, **118**, 728-744.

Chong, M., G. Jaubert, and M. Nuret, 1991: Small mesoscale structure of a cold–frontal rainband. *25 th Int. Conf. on Radar Meteor.*, 181–184.

Clough S. A., and Testud J., 1988: The FRONTS 87 experiment and mesoscale frontal dynamics project, *WMO Bull*, **37**, 276–281.

Gallus W.A. Jr, and R.H. Johnson, 1991: Heat and moisture budgets of an intense midlatitude squall line. *J. Atmos. Sci.*, **48**, 122-146..

Hoskins, B.J., and F.P. Bretherton, 1972: Atmospheric frontogenesis models: Mathematical formulation and solution. *J. Atmos. Sci.*, **29**, 103–122.

Houze, R. A., Jr., 1982: Cloud clusters and large-scale vertical motions in the tropics. *J. Meteor. Soc. Japan*, **60**, 396-410.

Houze, R. A., Jr., 1987: Observed structure of mesoscale convective systems and implications for large-scale heating. *Proceedings of workshop on diabatic forcing*, ECMWF.

Houze, R. A., Jr., 1989: Observed structure of mesoscale convective systems and implications for large-scale heating. *Quart. J. Roy. Meteor. Soc.*, **115**, 425-461.

Jaubert G., M. Nuret, and M. Chong, 1991: A case study of cold–frontal rainbands. *25 th Int. Conf. on Radar Meteor.*, 185–188.

Johnson, R. H., 1976: The role of convective-scale precipitation downdrafts in cumulus and synoptic scale interactions. *J. Atmos. Sci.*, **33**, 1890-1910.

Johnson, R. H., and G. S. Young, 1983: Heat and moisture budgets of tropical mesoscale anvil clouds. *J. Atmos. Sci.*, **40**, 2138-2147.

Johnson, R. H., 1984: Partitioning tropical heat and moisture budgets into cumulus and mesoscale components: Implications for cumulus parameterization. *Mon. Wea. Rev.*, **112**, 1590-1601.

Lafore, J.-P., J.-L. Redelsperger and G. Jaubert, 1988: Comparison between a three-dimensional simulation and Doppler radar data of a tropical squall line: Transports of mass, momentum, heat, and moisture. *J. Atmos. Sci.*, **45**, 3483-3500.

Lafore,J.P., and M.W. Moncrieff, 1989: a numerical investigation of the organization and interaction of the convective and stratiform regions of tropical squall lines. *J.Atmos.Sci.*,**46**,521-544.

Leary, C.A., and R.A. Houze, 1980: The contribution of mesoscale motions to the mass and heat fluxes of an intense tropical convective system. *J. Atmos. Sci.*, **37**, 784–796.

LeMone M.A., J. Fankhauser, and T. Matejka, 1990: Momentum generation and redistribution in convective bands: what have we learned?. *4th Conf. on Mesoscale Processes*, 198–199.

LeMone, M.A., G.M. Barnes, and E.J. Zipser, 1984: Momentum flux of cumulonimbus over the tropical oceans. *J. Atmos. Sci.*, **41**, 1914–1932.

Matejka, T., and M.A. LeMone, 1990: The generation and redistribution of momentum in a squall line. *4th Conf. on Mesoscale Processes*, 196–197.

Moncrieff, M.W., 1981: A theory of organized steady convection and its transport properties. *Quart. J. Roy. Meteor. Soc.*, **107**, 29–50.

Moncrieff, M.W., and D.W.K. So, 1989: A hydrodynamic theory of conservative bounded density currents. *J. Fluid Mech.*, **198**, 177-197.

Rotunno, R., J.B. Klemp, and M.E. Weisman, 1988: A theory of strong long–lived squall lines. *J. Atmos. Sci.*, **45**, 463–485.

Reed, R. J., and E. E. Recker, 1971: Structure and properties of synoptic-scale wave disturbances in the equatorial western Pacific. *J. Atmos. Sci.*, **28**, 1117-1133.

Redelsperger, J–L., and G. Sommeria, 1986: Three–dimensional simulation of a convective storm: Sensitivity studies on subgrid parameterization and spatial resolution. *J. Atmos. Sci.*, **43**, 2619–2635.

Redelsperger, J.L., and J.P. Lafore, 1988: A three-dimensional simulation of a tropical squall line: convective organization and thermodynamic vertical transport. *J.Atmos.Sci.*,**45**,1134-1356.

Smull, B.F., and R.A. Houze, 1987: Dual–Doppler radar analysis of a mid–latitude squall line with a trailing region of a stratiform rain. *J. Atmos. Sci.*, 44, 2128–2148.

Sommeria, G., and J. Testud, 1984: COPT 81: A field experiment designed for the

study of dynamics and electrical activity of deep convection in continental tropical regions. *Bull. Amer. Meteor. Soc.*, **65**, 4–10.

Tao, W.-K., and S.-T. Soong, 1986: A study of the response of deep tropical clouds to mesoscale processes: Three-dimensional numerical experiments. *J. Atmos. Sci.*, **43**, 2653-2676.

Thorpe, A.J., and S.A. Clough, 1991: Mesoscale dynamics of cold fronts – Part I: Structures described by dropsoundings in Fronts87. Submit to Quart. J. Roy. Meteor. Soc.